CHEMICAL REVIEWS

Review

Cite This: Chem. Rev. 2018, 118, 7867−7885

pubs.acs.org/CR

Capillary Electrophoresis Separations of Glycans

Grace Lu, Cassandra L. Crihfield, Srikanth Gattu, Lindsay M. Veltri, and Lisa A. Holland*

C. Eugene Bennett Department of Chemistry, West Virginia University, Morgantown, West Virginia 26506, United States

ABSTRACT: Capillary electrophoresis has emerged as a powerful approach for carbohydrate analyses since 2014. The method provides high resolution capable of separating carbohydrates by charge-to-size ratio. Principle applications are heavily focused on *N*-glycans, which are highly relevant to biological therapeutics and biomarker research. Advances in techniques used for *N*-glycan structural identification include migration time indexing and exoglycosidase and lectin profiling, as well as mass spectrometry. Capillary electrophoresis methods have been developed that are capable of separating glycans with the same monosaccharide sequence but different positional isomers, as well as determining whether monosaccharides composing a glycan are alpha or beta linked. Significant applications of capillary electrophoresis to the analyses of *N*-glycans in biomarker discovery and biological therapeutics are emphasized with a brief discussion included on carbohydrate analyses of glycosaminoglycans and mono-, di-, and oligosaccharides relevant to food and plant products. Innovative, emerging techniques in the field are highlighted and the future direction of the technology is projected based on the significant contributions of capillary electrophoresis to glycoscience from 2014 to the present as discussed in this review.

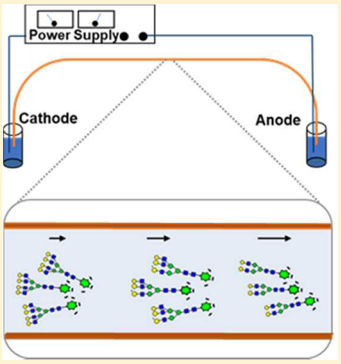

CONTENTS

1. INTRODUCTION

Carbohydrates are fundamental to signaling, structure, and energy. These molecules play important roles in renewable energy,[1] disease,[2−4] aging,[5] food,[6] and therapeutics.[7] The critical nature of glycans in signaling[8] supports the use for disease diagnosis, prognosis, and therapeutic intervention. Glycoscience encompasses a diverse range of applications such as mapping glycopeptides in protein targets or elucidating the role of glycosylation in signaling and ligand−receptor binding. Insight into the processes that lead to changes in glycosylation continues to become increasingly important in medical research[9] and biopharmaceutical manufacturing.[10] Glycosylation modulates biological activity[11] and strongly affects the antibody effector function. This holds the potential to dramatically improve drug performance[7] but requires enabling technologies, including capillary electrophoresis

Special Issue: Carbohydrate Chemistry

Received: November 7, 2017
Published: March 12, 2018

DOI: 10.1021/acs.chemrev.7b00669
Chem. Rev. 2018, 118, 7867−7885

(CE),[12,13] to monitor microheterogeneity throughout manufacturing.[13]

The interest in CE for glycoscience applications is evident by the recent high activity in published reviews in 2016 and 2017 alone.[14−18] This review focuses on the analysis of released oligosaccharides as a means to highlight the dynamic and rapidly evolving advances in CE instrumentation and methodology. In 2015, several industrial and academic laboratories participated in an interlaboratory test, which involved an *N*-glycan mapping exercise with a protein test sample and demonstrated good reproducibility in area and migration time.[19] Currently, commercial kits have made use of the technology more routine in industry by streamlining sample preparation for higher throughput.[20−24] These advances are serendipitous as a healthy rate of growth is expected for the antibody pharmaceutical market, which is estimated to reach an annual global value of $125 billion USD in 2020.[25] This creates an even more pressing need for high throughput analyses, which can be met by CE.

There are several advantages of CE. High electric field results in short separation times and high efficiency, in the absence of Joule heating.[26] Injected sample volumes are in the femtoliter to nanoliter range. Only a few milliliters of running buffer are required for a 24-h period. Separations performed on commercial instruments are automated. Detection limits with laser-induced fluorescence are in the femtomolar range. Typical instruments contain a single capillary with temperature control of the capillary and solutions. Multiple capillaries can be used in a single instrument to increase the throughput. For example, instruments used for DNA sequencing can hold from 16 to 96 capillaries.[27−31] Injections can even be multiplexed to deliver packets of sample within a single run to eliminate dwell times.[32] Innovations in instrumentation and in applications of the methodology continue and can be observed as a push to make the technique more accessible to researchers through commercially available solutions to interfacing CE with a mass spectrometer, as well as databases and software that increase the ease of data analysis. Analytical techniques are continually adapted to meet the growing challenges in carbohydrate analysis and CE plays a unique role in glycoscience research.

This review is an exhaustive update of the most recent activity in CE glycoscience applications, covering advances from 2014 through 2017. Recognizing that the field is multidisciplinary, attention is given to fundamental principles of glycan structure as well as CE separations. Advances in labeling and the development of highly automated, high throughput methods of sample preparation are noted. Substantial consideration is given to the three primary approaches to identifying glycan peaks, including migration time indexing, enzyme or lectin profiling, and mass spectrometry (MS). A discussion of advances in labeling and in particular in creating highly automated high throughput methods of sample preparation is included. A focus is placed on cutting edge applications and technologies. A review of applications for biomarker discovery, characterization of therapeutics, and applications to food and pathogen analyses is given. The report concludes with areas of emerging CE technologies that will have a long and sustaining effect in the field of glycosciences with further development.

2. BACKGROUND

2.1. Carbohydrate Fundamentals

It is easier to appreciate the analytical challenges associated with carbohydrate analyses by considering the complexity of carbohydrate structures. A brief description is presented in this review, which centers on factors important to CE. Other sources may provide additional information regarding a detailed description of glycan nomenclature and structure,[33] as well as an overview of different nomenclature and fragmentation patterns observed in MS.[34]

Monosaccharides, which are the building blocks for polysaccharides such as glycans and glycoforms, can be roughly classified to contain an empirical formula of $(C_x(H_2O)_n)$. A vast array of different monosaccharides exist,[35] but for the purposes of this review, only 6 structures are presented in Figure 1 to

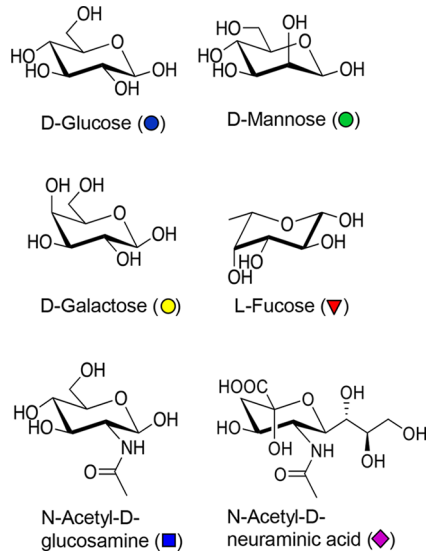

Figure 1. Six representative structures of D conformer monosaccharides. Glucose, mannose, and galactose are common unsubstituted hexose saccharides. Fucose has one less hydroxyl group and is termed a deoxy-hexose sugar. *N*-Acetylglucosamine and *N*-acetylneuraminic acid represent substituted hexose saccharides.

demonstrate the subtle differences in these structures. The position of the hydroxyl substituents is the only difference among hexose saccharides: mannose, glucose, and galactose. Examples of substituted hexose saccharides include *N*-acetylneuraminic acid and *N*-acetyl glucosamine. Fucose is an example of deoxy-hexose saccharide.

Polymerizing these saccharide monomers dramatically increases the structural diversity, as well as the complexity of carbohydrates. Oligosaccharides and polysaccharides can vary by the monomer structure. The linkage orientation can be alpha or beta, and the position of the linkage can differ, as shown in the trisaccharides depicted in Figure 2. Although the known biosynthetic pathways of classes of oligosaccharides limit the variety of structures that are physiologically relevant, a range of diverse carbohydrate structures occur, which is why these molecules play a substantial part in signaling. A consequence of this diversity is that isomeric structures are not only possible but highly probable. Amidst this complexity in carbohydrate structure, other repeating structural motifs have been classified. This includes linear polysaccharides composed of repeating disaccharide units that are glycosaminoglycans

DOI: 10.1021/acs.chemrev.7b00669
Chem. Rev. 2018, 118, 7867−7885

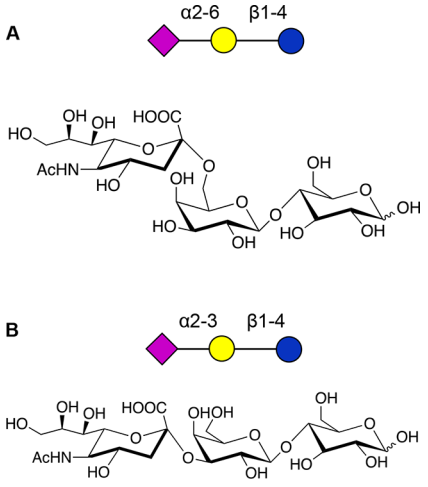

Figure 2. Two structures of sialyllactose that differ only by the linkage between the sialic acid and galactose monosaccharides. The structure in panel A is 6′-sialyllactose, which is composed of an α2−6 linkage. The structure in panel B is 3′-sialyllactose, which is composed of an α2−3 linkage.

(mucopolysaccharides). This class of polysaccharides, which plays various roles in life including motor function, cell growth, and anticoagulation, is composed of many familiar molecular classes such as heparin/heparan sulfate, chondroitin/dermatan sulfate, hyaluronic acid, and keratin sulfate.

A predominant class of carbohydrates in biomarker research and biological therapeutics are asparagine-linked carbohydrates or *N*-glycans. Serine and threonine glycans (*O*-glycans) also exist, but their analyses by electrophoresis has not accelerated to the same degree as seen for *N*-glycans owing to difficulties associated with glycan labeling via reductive amination following chemical release of the glycan by β-elimination. The common feature of N-linked glycans is a core structure composed of a combination of *N*-acetylglucosamine residues and mannose residues as shown in Figure 3.[33] Complex *N*-

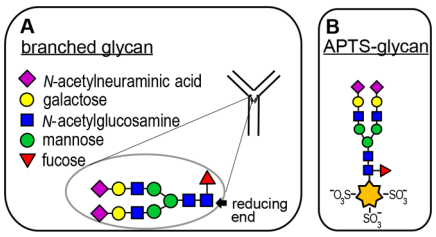

Figure 3. Depiction of an *N*-glycan, which is composed of several monosaccharides, removed from an antibody. The reducing end (B), which is located where the *N*-acetylglucosamine is cleaved from the antibody, is the target for the attachment of fluorophores, such as APTS.

glycans vary by the presence of fucose, galactose, additional branching and bisecting *N*-acetyl glucosamine, sialic acid capping, and other modifications such as polylactosamine capping. Although *N*-glycans represent only a single category of carbohydrates, there is a strong focus on these structures in CE because they are a post-translational modification with heavy implications in physiological function. This makes *N*-glycans powerful for biomarker discovery and for practical applications in biological therapeutics. In spite of the complexity and diversity of *N*-glycan structures, *N*-glycan labeling is simplified by targeting the reducing end of polysaccharide structures, as shown in Figure 3. This ensures the molecules are labeled with a single fluorophore using standard reductive amination. The addition of a charged tag on the *N*-glycan structure is serendipitously compatible with CE.

2.2. Capillary Electrophoresis Fundamentals

Capillary zone electrophoresis separations are well-suited to biomolecular separations because the method is based on transport in an electric field.[36] Electroosmotic flow (EOF) and electrophoretic mobility are the two transport mechanisms that are fundamental to CE. EOF is the bulk flow of the background electrolyte. In a bare fused silica capillary EOF moves from the anode toward the cathode due to the negative surface charge of the capillary and the presence of the electric field. Electrophoretic transport is a function of charge-to-size ratio. Analyte is attracted to either the anode or cathode and the size of the molecule determines the speed of transport. These two modes of transport are superimposed in most CE separations. In a CE separation with the anode at the site of injection in a bare fused silica capillary, when EOF is present the order of analyte migration is small positively charged molecules, larger positively charged molecules, comigrating neutral molecules, large negatively charged molecules, and smaller negatively charged molecules.

Separations of carbohydrates by CE are unique because a majority of saccharides are uncharged, except glycans containing acidic sugars (e.g., *N*-acetylneuraminic acid, glucuronic acid, or iduronic acid). Additionally, carbohydrate molecules lack a chromophore and cannot be detected with absorbance detection in the UV range. These confounding factors are addressed by labeling the carbohydrates with a fluorophore. The fact that most fluorophores are charged is an advantage in CE because it ensures that the labeled carbohydrate migrates in the electric field. The fluorescent label 8-aminopyrene-1,3,6-trisulfonate (APTS) was among the first dyes reported for oligosaccharide analyses with CE[37] and has an excitation maximum near the 488 nm line of an argon ion laser. Labeling with APTS, which is shown in Figure 4, has been well established.[38−40] Covalent modification of oligosaccharides by reductive amination produces singly labeled product at nearly 100% labeling efficiency.

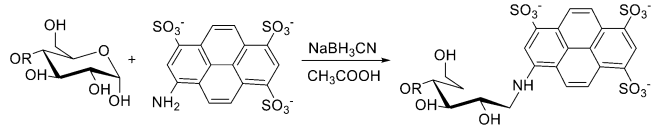

Figure 4. Simplified mechanism of reductive amination as it is used to label carbohydrates with APTS using a reducing agent (sodium cyanoborohydride).

Once labeled glycans are negatively charged, the separation is adjusted to rely on electrophoretic transport to accentuate differences in charge-to-size ratio. As depicted in Figure 5, neutral glycans harbor three additional negative charges following conjugation to APTS. Sialylated glycans labeled with APTS are even more negative and as a result have an even faster migration. The EOF is suppressed by eliminating the surface charge on the capillary wall through surface modification. The electric field is applied under reversed polarity to drive anions toward the detection window. Using the simplest relationship between molecular weight and

DOI: 10.1021/acs.chemrev.7b00669
Chem. Rev. 2018, 118, 7867−7885

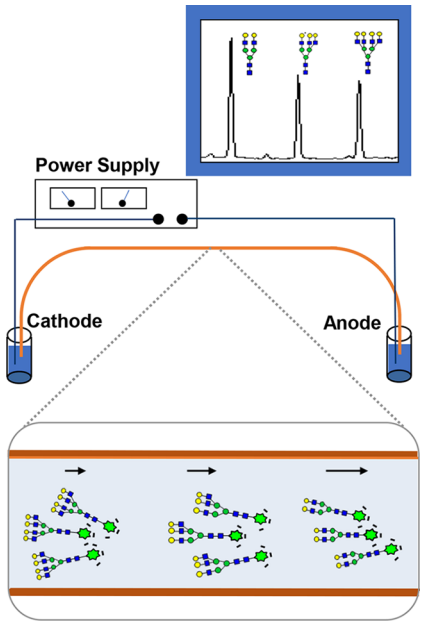

Figure 5. Basic diagram of the capillary electrophoresis system commonly used to separate APTS-labeled glycans. Separations are performed in reverse polarity (cathode to anode) under suppressed electroosmotic flow using a coated capillary. APTS-labeled glycans are separated by charge-to-size ratio in the order of ascending hydrodynamic volume as shown in the inset and quantified using an electropherogram generated by laser-induced fluorescence.

molecular size, the electrophoretic mobility, μ_{eph}, is a function of molecular size as described in eq 1

$$\mu_{eph} = q/6\pi\eta r \quad (1)$$

where q is the charge, η is the viscosity of the background electrolyte, and r is the hydrodynamic radius of the molecule.[41]

Viscosity plays a role in frictional drag (see eq 1) and is one strategy to achieve the high resolution needed to distinguish oligosaccharide isomers. Additives are often included in the background electrolyte to improve resolution. The carbohydrate separation mechanism facilitated by the use of linear gels is solely based on charge-to-size ratio and is not size-based sieving, which is observed for larger biomolecules such as proteins and DNA.[42] As it is applied to carbohydrate analyses, the separation technique has been interchangeably referred to as CE or capillary gel electrophoresis when a gel is included in the background electrolyte. Fluorophore assisted carbohydrate electrophoresis has also been used, although this nomenclature can be misleading as the method may be accomplished using slab gel[43,44] as well as CE.[45]

2.3. Performance of Capillary Electrophoresis Relative to Other Methods

A variety of analytical tools are used significantly in glycosciences including chromatography,[18,46] mass spectrometry,[18,46−48] ion mobility,[18,47] and lectin arrays,[48] and CE has developed into a powerful approach to complement existing technology. In 2014, Huffman et al. reported a comprehensive assessment of the use of CE relative to reversed phase chromatography coupled with fluorescence detection matrix assisted laser desorption ionization-time-of-flight MS versus liquid chromatography−electrospray ionization−MS. Each of these techniques was evaluated by measuring *N*-glycans from IgG molecules in plasma samples from 1201 individuals.[30] The purpose of this study was to establish the benefits of these available technologies since focusing on particular technologies affects the findings of large scale studies as well as the resource investment. Several important advantages of CE were identified by the authors. First, the high resolution of CE enabled isomer separation and linkage analysis. Second, quantification was achievable only with CE and the liquid chromatography method coupled to fluorescence detection. Third, by using instruments with 16-capillary arrays, the authors achieved extraordinary throughput relative to both liquid chromatography methods. The cost of the CE instrument, as reported by the authors was on par with that of liquid chromatography and with low-end MS approaches. The authors noted that the CE method offered substantially reduced cost per sample. Limitations identified by the authors included poor acceptance by the glycomics community and the lack of a large structural database.

Other reports have compared the performance of CE to separation techniques used to analyze *N*-glycans. Reusch et al. compared the performance of capillary gel electrophoresis with fluorescence detection against hydrophobic interaction liquid chromatography (HILIC) separations coupled with fluorescence using two different labels, demonstrating good agreement among these approaches as well as the advantage of CE to separate positional isomers.[27] A complementary study compared CE with fluorescent detection to anion exchange with pulsed amperometric detection and HILIC with fluorescent detection, which served as the reference.[49] Different modes of CE were evaluated including capillary zone electrophoresis (separations in the presence of EOF), capillary gel electrophoresis (separations under reversed polarity with suppressed EOF and a gel additive), and DNA fluorophore assisted CE (capillary gel electrophoresis at an elevated temperature using a genetic analyzer). The authors indicated only minor differences in accuracy, precision, and separation performance.[49]

Comparisons of separation-based methods for *N*-glycan analyses using significantly larger sample sets to evaluate a wider range of glycosylation present on IgG antibodies were also reported. Adamczyk et al. explored the differences in separation based approaches of CE, reversed phase liquid chromatography, and HILIC by comparing the results obtained for therapeutic IgG Fc-glycosylation profiles from different healthy mammalian species.[50] The results of their work demonstrated that CE and HILIC had similar performance and were both better suited to resolve complex mixtures than reversed phase liquid chromatography.[50] In a separate report, Mahan et al. compared capillary gel electrophoresis to HILIC demonstrating that while both methods yield comparable results, electrophoresis was more cost-effective, consumed less sample, and was operated with higher throughput.[29] The authors demonstrated that the method was suitable to identify differences in glycosylation profiles for Fab fragments from polyclonal antibodies expressed within species and that glycosylation profiles are dramatically different across human, rhesus, and mouse.[29]

3. CARBOHYDRATE DERIVATIZATION

3.1. Advances in Labeling

Glycan labeling with APTS remains the method of choice for CE separations.[19,27,29,31,40,50−73] Glycan labeling with APTS through reductive amination is well-established and is preferred

DOI: 10.1021/acs.chemrev.7b00669
Chem. Rev. 2018, 118, 7867−7885

over other strategies, including Michael addition or hydrazide[74] or oxime formation.[75] A recently reported modification of reductive amination chemistry is the use of catalysts to facilitate the direct transfer of hydrogen.[57] The use of catalysts is important to automated parallel processing and subsequently high throughput because it obviates the generation of hydrogen cyanide formed using sodium cyanoborohydride in the presence of acid.

In addition to APTS, other labeling reagents can be used with CE separations of carbohydrates. Recently, 2-amino-benzoic acid was used with a helium cadmium laser rather than an argon ion laser,[76] as well as for UV−visible absorbance detection[77] or CE coupled with MS.[78] The fluorescent label 7-amino-4-methylcoumarin[79] was also reported with an UV light emitting diode excitation source. This dye is neutral following conjugation and labeling, so the use of boric acid, which complexes with diols to form a negative complex in order to separate glycans, was required.[80]

Despite the expansion of glycan analysis to the use of other dyes, APTS is still the most commonly utilized dye for glycan analysis by CE for several practical reasons. The fluorescence of the APTS labeled glycans is 40-fold higher than that of unconjugated APTS.[37] Additionally, the background interference from biomatrices can be reduced because the excitation wavelength of APTS is in the visible range (λ_{ex} = 488 nm), whereas the other dyes are excited in the ultraviolet range, 2-amino benzoic acid (λ_{ex} = 325 nm) and 7-amino-4-methylcoumarin (λ_{ex} = 354 nm).

3.2. Analytical Technology To Improve Sample Processing

Given the significance of antibody therapeutics and a clear need to assess glycosylation on a high throughput scale, the enzymatic and chemical steps performed in research laboratories to deglycosylate, label, and purify samples are a bottleneck to routinely implementing CE separations in pharmaceutical processing. Serious effort has been invested in automating these sample handling steps required to achieve the labeled glycan products. Purification of antibody therapeutics from crude lysate using Protein A extraction cartridges and labeling are accomplished with a combination of commercial products or with complete kits.[63] Other efforts to increase throughput include different strategies to immobilize the enzyme or glycan during processing.

Prior to analysis, N-linked glycans are typically released from glycoproteins enzymatically, although methods of chemical release have recently been described based on simple oxidative release with sodium hypochlorite.[81] PNGase F, the enzyme commonly used for the release of *N*-glycans, has been immobilized using commercially available glutathione resin and a glutathione S-transferase fusion protein of PNGase F.[65] The authors demonstrated faster reaction kinetics for the immobilized enzyme and complete turnover for both immobilized and free solution PNGase F.[65] These automated steps have been fully integrated with a Biomek FX^P Laboratory Automation Workstation.[64]

Different commercial kits are available to prepare glycans with improved workflow.[20−24] Automated processing for labeling continues to advance beyond the use of HILIC extraction cartridges to purify labeled glycans. Magnetic beads (Agencourt Cleanseq magnetic beads from AB Sciex) have been used to automate 5 serial steps of labeling.[40] The commercial beads are manufactured to contain carboxylic acid functional groups. During deglycosylation, the glycone is liberated as a positively charged glycosylamine. This glycone product ion pairs with the carboxylic acid beads and is easily separated from the spent enzyme reaction and cleanly transferred to solution ideal for APTS labeling. During purification, the reaction solution is diluted to contain a high acetonitrile composition (80%). Under this condition, the beads support hydrophilic interaction, retaining glycans due to molecular crowding. An alternative strategy to purify labeled glycans from the labeling process utilizes solid phase extraction materials. A fritless in-line solid phase extraction device was designed that coupled large diameter anion exchange packing material into the separation by sandwiching the material between two narrow inner diameter capillaries.[70] The in-line fritless cartridge was used to enrich anionic samples prior to the CE separation and was successfully applied to APTS-labeled glycans.[70] Finally, slab gel electrophoresis was reported for glycan purification by excising gels and extracting the labeled glycans.[51]

4. METHODS TO IDENTIFY GLYCANS

Several methods have been developed in an effort to identify the structure and linkage composition of unknown glycans in samples. These techniques fall into the broad categories of calibration of migration time with ladders and standards, exoglycosidase and lectin reactions, and MS analysis. This section details the fundamentals and recent advances of these techniques as they are critical to glycan identification in current and emerging technologies.

4.1. Calibration of Migration Time with Ladders and Standards

CE utilizes a migration time index for glycan identification. Briefly, the migration of the analyte is best referenced to a size ladder generated by a homologous series of a linear glucose polymer.[82] Some aspects of the separation introduce variability in the migration time, which can be accounted for using a size ladder as a standard. The apparent mobility of the analyte is the sum of the electrophoretic mobility and bulk EOF. Although the EOF is suppressed, a small component is present and will change from run to run with any changes in the surface characteristics of the capillary wall. Adsorption of biomolecules to the surface, a change in the ionic strength of the background electrolyte, or variation in the pH, for example, due to electrolysis in the anodic and cathodic reservoir, will contribute to this modest variability in EOF. Referencing the analyte to the ladder solves any issues with reproducibility in the migration time. Glucose unit (GU) values have been used to quantify the impact of the number of monosaccharides and the monosaccharide linkage in CE separations and to estimate the unknown glycan structure (hydrodynamic size) as early as 1996,[83,84] with a series of improvements being published.

The approach is identical to the use of Kovat's index as a referencing tool in gas chromatography. Indexing migration time improves the reproducibility of separations based on the same method. It also is effective for comparing migration times across separations performed with different methods, as was demonstrated for different field strengths, effective separation lengths, separation temperatures, surface coatings, and injection modes.[85] Traditionally, a complete glycan ladder is used to estimate the relative size of the sample using the migration time of the standard oligomer and the analytes to address an experimentally observed change in ladder migration associated with a helical turn that occurs in maltooligosaccharide

DOI: 10.1021/acs.chemrev.7b00669
Chem. Rev. 2018, 118, 7867−7885

structures above a degree of polymerization of 7.[85] However, as shown in Figure 6, the approach is simplified to only three co-

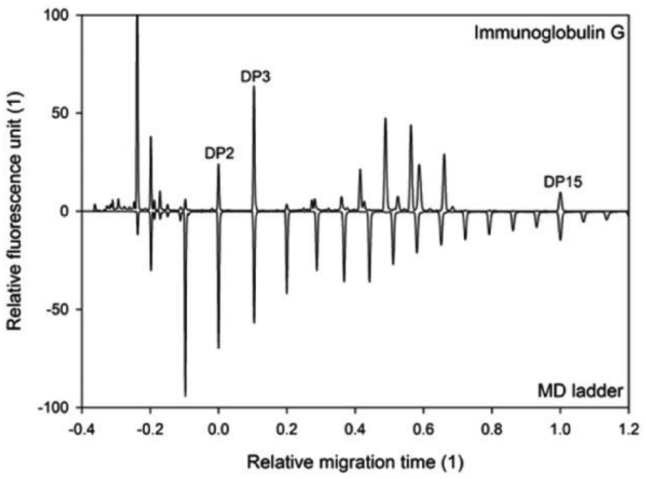

Figure 6. Electropherogram of three internal standards (DP2, DP3, and DP15 are maltose, maltotriose, and maltopentadecaose, respectively) and APTS labeled N-linked glycan released from human immunoglobulin G in the upper trace. The representative electropherogram of maltooligomers in the lower trace is aligned with DP2, DP3, and DP15 in the upper panel. Reprinted with permission from ref 85. Copyright 2016 American Chemical Society.

injected size standards to accurately index migration time without the drawbacks of ladder and sample overlap due to comigration.[85] Additionally, one standard also serves to normalize variations in the sample injection.[85]

The calculation of the GU value is straighforward.[56] As shown in eq 2, the glucose index of the specified glycan analyte, GU_x

$$GU_X = G_N + \frac{t_X - t_N}{t_{N+1} - t_N} \quad (2)$$

where G_N is the number of maltose in the adjacent maltooligosaccharide ladder peak, t_X, t_N, and t_{N+1} are the migration times of the target glycan and the N and $N + 1$ number of maltooligomers, respectively. The use of a glycan ladder and GU values was further improved with the built-in database GUcal for high throughput analysis,[56,85] reported as www.gucal.hu.[86] The program automatically calculates the GU values of peaks in the electropherogram upon loading the ASCII file of both standard maltooligosaccharide ladder and sample traces.

GU values are also applied to evaluate the impact of temperature on hydrodynamic size of both linear and branched *N*-glycans using CE.[54,87] The experimental results showed that GU values changed as a function of temperature from 20 to 50 °C using background electrolytes prepared with or without linear polymer additives. The temperature dependence of the GU values is attributed to the difference in activation energy for linear and branched glycans, which is 0.4 and 1.5 J/mol/Å^3, respectively.[54] The concept of exploiting differences in the activation energy of different glycan structures by changing separation temperature was utilized to optimize the resolution achievable for *N*-glycans of biotherapeutic interest.[87]

Furthermore, the virtual maltooligosaccharide ladder was developed using a triple-internal standard approach in order to circumvent interference when co-injecting the glycan ladder with target analytes or the need to perform a separate run for the standard glycan ladder. These three internal standards include maltose (DP2), maltotriose (DP3), and maltopentadecaose (DP15). The DP3 was added to the cleaved *N*-glycans in order to estimate labeling as well as the injection efficiency. This enabled its use as an internal standard as well as a migration standard. The APTS labeled DP2 and DP15, which were not included in the sample reaction, bracketed the target analyte in the electropherograms without overlapping with the glycan peaks. The virtual glycan ladder from DP2 to DP7 was estimated using the migration time difference between the two injected standards, GU_{DP2} and GU_{DP3}. The ratio of the migration time differences between two consecutive peaks (DP < 7) to DP2 and DP3 was reproducible (RSD < 1%). On the other hand, the GU values for oligosaccharides with more than 7 glucoses (DP8−DP15) were evaluated using the migration time of DP15 in the sample traces because maltooligosaccharides with more than 7 glucoses form helical structures, and the migration time differences between two consecutive oligomers remain constant.[82] Therefore, the virtual ladder, as well as the injection efficiency, can be estimated using the triple-internal standard.

High precision of the measured GU values obtained from the triple-internal standard approach allows identification and prediction of the structures based on a direct comparison of GU values between known standards and the unknown glycan. The *N*-glycan profile of formalin-fixed paraffin-embedded mouse tissue samples was identified using the combination of exoglycosidase and the GU values.[58] The sample included neutral and mono- and disialo *N*-glycans. The presence of terminal sialic acid, carrying one negative charge, led to shorter migration times. Therefore, GU values in the range of 4−6, 7−9, and 9−13 indicate disialo, monosialo, and neutral *N*-glycans, respectively. The *N*-glycan patterns after exoglycosidase treatment were identified using GU value and a publicly accessible database.

An alternative platform to analyze *N*-glycan sequence using multiplexed capillary gel electrophoresis was developed based on a DNA sequencing instrument. Software glyXtool[30,66,88] and glyXalign[30,89] were developed for *N*-glycan analyses in order to address issues with shifts in migration time and peak assignment. GlyXalign and glyXtool identify the peaks and align the electropherograms based on the internal standard, which is composed of single-stranded DNA fragments ranging

Table 1. Examples of Commercial Exoglycosidases

monomer	enzyme linkage selectivity
N-acetylneuraminic acid	*N*-acetylneuraminidase: α2−3, α2−3,6, α2−3,6,8, α2−3,6,8,9
galactose	galactosidase: β1−3, β1−4, β1−3,4, β1−3,6, β1−4,6
N-acetylglucosamine	*N*-acetyl-glucosaminidase: β1−2,3,4,6
mannose	mannosidase: α1−2, α1−2,3, α1−6, α1−2,3,6
fucose	fucosidase: α1−2, α1−6, α1−3,4, α1−2,4,6, α1−2,3,4,6

DOI: 10.1021/acs.chemrev.7b00669
Chem. Rev. 2018, 118, 7867−7885

in size from 35 to 500 bases (GeneScan-500 LIZ Size Standard). As a result, high throughput analysis for *N*-glycan identification was achieved and applied for diagnostic purposes.[88]

4.2. Identification with Exoglycosidases and Lectins

4.2.1. Identification with Exoglycosidases. Exoglycosidases are enzymes that cleave an oligosaccharide residue from the nonreducing end of a glycan, proteoform, or oligosaccharide (see Figure 3). These enzymes are selective for specific oligosaccharide monomers. The enzyme may have additional selectivity, for example, for the linkage orientation (α vs β) or the position of the carbon−carbon linkage (e.g., α2−3 vs α2−6 sialic acid as shown in Figure 2). Conversion of a carbohydrate by an exoglycosidase is only possible if the exoglycosidase specificity matches the characteristics of the terminal monomer. As summarized in Table 1, a number of exoglycosidases are commercially available with different specificity. The conversion of substrate to product is harnessed with CE by analyzing the carbohydrate before and after enzyme treatment. The formation of product is observed as a shift in migration time. This is depicted conceptually in Figure 7A, where galactosidase

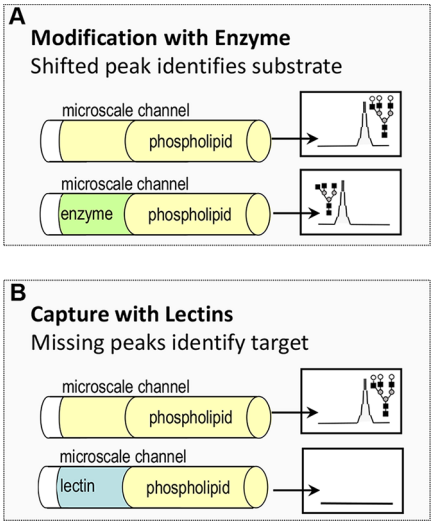

Figure 7. Conceptual diagrams of online enzyme and lectin reactions in-capillary. Panel A depicts a galactosylated triantennary glycan separated in the absence and presence of galactosidase. Upon cleavage of the terminal galactose residues, the glycan migrates faster due to mass loss. Panel B depicts galactosylated triantennary glycan in the absence and presence of *Erythrina cristagalli* lectin. Upon binding to the terminal galactose residues, the glycan is not detected.

enzyme cleaves terminal galactose residues from an *N*-glycan. It is possible to elucidate the sequence and linkage of oligosaccharides following treatment with appropriate exoglycosidases. These analyses are performed off-line or online with the CE.

The benefit of modifying *N*-glycan samples prior to CE separations using enzymes was recognized early.[90] Applications with CE have been performed off-line with a variety of enzymes[28,59,88,91] and typically focus on removal of sialic acids[52,66,92] in some cases as a means to reduce complexity of the CE separation.[92] These reactions are typically performed overnight at an elevated temperature and a specified pH. Other considerations for off-line reactions include vendor added stabilizers or other additives with the potential to interfere with different aspects of the analysis. The formation of sodium adducts or introduction of nonvolatile salts is a concern for CE separations coupled with MS. The potential for some exoglycosidase enzymes to exhibit transferase activity, reattaching the liberated monomers to the product, can be alleviated with in-line reactions. Optimized reaction conditions with long incubation times allow the use of lower amounts of enzyme, which can be important for expensive enzymes, such as those with high specificity. This also accounts for differences in reaction rates inherent with different substrates. For example, neuraminidase derived from *Clostridium perfringens* (*C. welchii*) exhibits higher rates of cleavage dependent upon the neuraminidase linkage with α2−3 > α2−6 > α2−8. This is in contrast to rates observed with neuraminidase derived from *Arthrobacter ureafaciens* or from *Vibrio cholera,* which exhibit cleavage rates of α2−6 > α2−3 > α2−8.

Exoglycosidases can also be integrated into the CE separation to streamline carbohydrate identification, reducing the amount of enzyme as well as the time required for enzymatic conversion. This was recently utilized as a means to quantify the rate of enzymatic cleavage as the Michaelis−Menten constant. Michaelis−Menten constants are determined by measuring the rate of product formation at different substrate concentrations. A plot of the reaction velocity against substrate concentration generates a hyperbolic curve. The substrate concentration that produces the half-maximal reaction velocity is the Michaelis−Menten constant. Neuraminidase enzymes with different sialic acid linkage specificity were evaluated for Michaelis−Menten constants for α2−3 versus α2−6 sialyllactose.[77] As measurement requires that the substrate concentration is on the order of the Michaelis−Menten constant, analyses of neuraminidase required the carbohydrates to be labeled with a UV−visible active tag (2-amino benzoic acid). This facilitated the use of substrate concentrations ranging from 0.4 to 7.4 mM, producing quantifiable levels of the lactose product.

With knowledge of the Michaelis−Menten constant, the method of in-line enzymatic sequencing was used to evaluate complex *N*-glycans. These studies were accomplished with fluorescent detection of APTS-labeled *N*-glycans, which made the method applicable to nanomolar *N*-glycan samples. Unique to this study was the use of a thermally reversible nanogel to pattern the enzyme in specific locations in the separation capillary either in aqueous background electrolyte or in capillary filled entirely with nanogel. Substrate was driven through the nanogel, and incubation was controlled electrophoretically by repeatedly applying voltage in forward and reverse polarity in order to cycle the analyte through the region of the capillary that contained enzyme. The study demonstrated a means to extend the lifetime of enzyme preparations at low concentration from a few hours to over 1-month.[77] Exoglycosidase with high specificity for α2−3 sialic acid linkages was used to evaluate the relative composition of sialic acid linkage. A significant finding of this work is that the enzyme considered general for α2−3 and α2−6 sialic acid could also be used to quantify the relative composition of sialic acid linkage by harnessing the lower reaction rate observed for α2−6 linkages as compared to α2−3 linkages. This resulted in substantial cost savings as enzymes with linkage specificity are more expensive than enzymes that cleave a particular saccharide residue regardless of linkage. The use of nanogel to pattern enzyme was extended to galactosidase in order to distinguish terminal galactose with a β1−3 versus β1−4 linkage in complex *N*-glycans.[93] Again, mixing during the

DOI: 10.1021/acs.chemrev.7b00669
Chem. Rev. 2018, 118, 7867−7885

reaction was provided via polarity switching. This strategy allows exquisite control of the ratio of enzyme to substrate, the incubation time, and reagent mixing, while also providing a practical strategy to sustain the enzyme activity in a cost-effective manner. These applications are significant because linkage position holds potential to serve as a biomarker and CE can complement other technologies that identify linkage with mass spectrometry through derivatization and fragmentation analyses,[18,94] as well as separation via liquid chromatography[95] or ion mobility.[18,47,94]

The advantages associated with in-capillary enzymolysis can be realized with a number of exoglycosidases. Yamagami et al. demonstrated the utility of five different exoglycosidases: β-galactosidase, α-mannosidase, β-acetylhexosaminidase, α-neuraminidase, and α-fucosidase for *N*-glycan identification.[96] These in-line enzyme reactions were accomplished with limited enzyme volumes within the separation time. Electrophoresis was used to drive the substrate through the enzyme zone with mixing or stopped flow incubation, which is called zero potential mixing. The method enabled determination of glycosidic linkage in *N*-glycans cleaved from different glycoproteins.

4.2.2. Glycan Identification with the Use of Lectins. Lectins are glycan-binding proteins that recognize structural features such as neuraminic acids or high mannose content. The specificity of lectins varies; for example, *Sambucus nigra* lectin binds only to α2−6 neuraminic acids while *Maackia Amurensis* lectin binds only to α2−3 neuraminic acids. As summarized in Table 2, many other lectins exist and are commercially available with different specificities. Lectins are used for structural identification in CE by performing a separation in the absence and then the presence of the lectin in the background electrolyte. When a structural match is present, the lectin binds to the glycan, leading to a dramatic change in the charge-to-size ratio. As shown in Figure 7B, this is observed in the electropherogram as a peak that disappears. The versatility of this approach was reported by Kinoshita, through separations performed in the absence and presence of a single lectin added to the background electrolyte in each run.[97] A set of 14 different lectins were applied to *N*-glycans labeled with APTS or to milk oligosaccharides labeled with 2-aminobenzoic acid. These lectins, concanavalin A, wheat germ agglutinin, *Datura stramonium* agglutinin, *Aleuria aurantia* lectin, *Ulex europaeus* agglutinin, *Ricinus communis* agglutinin, soybean agglutinin, *Maackia amurensis* lectin, *Pseudomonas aeruginosa* A lectin, *Aspergillus oryzae* lectin, *Tulipa gesneriana* agglutinin, *Crocus sativus* lectin, *Rhizopus stolonifer* lectin, and *Rhizopus stolonifer*, were purchased or were purified from plants by the authors.

Table 2. Examples of Commercial Lectins

lectin class	preferred glycan signature[a]
Fucose Binding Lectin	
Aleuria aurantia lectin (AAL)	Fucα1−3,6
Aspergillus oryzae lectin (AOL)	Fucα1−6 (core)
Lotus tetragonolobus (LTA)	Fucα1−3
Ulex europaeus agglutinin I (UEA-I)	Fucα1−2
Galactose and *N*-Acetylgalactosamine Binding Lectin	
Erythrina cristagalli lectin (ECL)	Galβ1−4GlcNAc
Griffonia simplicfolia isolectin B_4(GSL I−B_4)	Galβ1−3GlcNAc
peanut agglutinin (PNA)	Galβ1−3GalNAc
Phaseolus vulgaris leucoagglutinin (PHA-L)	terminal Gal GlcNAcβ1−2,6Man (tri/tetraantennary)
Ricinus communis agglutinin (RCA)	Galβ1−4GlcNAc, GalNAc
Soybean agglutinin (SBA)	terminal Gal, GalNAc
N-Acetylneuraminic Acid Binding Lectins	
Maackia amurensis lectin (MAL)	NeuAcα2−3Galβ1−4GlcNAc
Sambucus nigra agglutinin (SNA)	NeuAcα2−6Gal(NAc)
N-Acetyl Glucosamine Binding Lectin	
Datura stramonium lectin (DSL)	GlcNAc
Phaseolus vulgaris erythroagglutinin (PHA-E)	bisecting GlcNAcβ1−4 terminal Gal (biantennary)
Solanum tuberosum (STL)	GlcNAc
wheat germ agglutinin (WGA)	GlcNAc
Glucose and Mannose Binding Lectins	
concanavalin A (Con A)	αMan, αGlc
Pisum sativum agglutinin (PSA)	αMan, αGlc

[a]Fucose (Fuc), galactose (Gal), *N*-acetylgalactosamine (GalNAc), glucose (Glc), *N*-acetylglucosamine (GlcNac), mannose (Man), *N*-acetylneuraminic acid (NeuAc).

An alternative to filling the entire capillary with lectin is to confine the lectin to a zone within the capillary using a thermally reversible nanogel. This strategy enabled the use of lectins and enzymes in series and was used to distinguish Galβ1−3GlcNAc from Galβ1−4GlcNAc linkages in *N*-glycans.[93] The advantage of this approach is that combinations of lectins and enzymes can create unique specificity that is difficult to realize with the lectins and enzymes that are currently available. In the report by Holland et al, an enzyme specific for β1−4 galactose residues was used in combination with *Erythrina cristagalli* lectin specific for β1−3,4 galactose residues.[93] Analysis of the *N*-glycan was accomplished with two zones, with the first zone containing β1−4 galactosidase and the second containing *Erythrina cristagalli* lectin. The enzyme cleaved the terminal galactose residues with a Galβ1−4GlcNAc linkage, leaving any Galβ1−3GlcNAc linkage intact. The *Erythrina cristagalli* lectin subsequently pulled down any *N*-glycan containing residual Galβ1−3GlcNAc linkages.

4.3. Structural Verification with MS

MS is used as a tool to complement CE separations for the identification of glycan structures. Matrix assisted laser desorption ionization[55,59,98−101] and electrospray ionization[91,98,102−105] are the most commonly employed ionization sources for *N*-glycan analysis. Matrix assisted laser desorption ionization methods relying on exact mass[59,98−100] and fragmentation[55,101] have been reported for the determination of *N*-glycan structure. These matrix assisted laser desorption ionization methods occur either entirely decoupled from the CE separation[55,59,99,100] or, as shown in Figure 8, with the CE instrument modified in order to spot eluent from the capillary onto a plate used for matrix assisted laser desorption ionization.[98,101] Alternatively, the electrospray ionization techniques occur almost exclusively in-line with the CE separation.[91,102−104] Sheathless interfaces that introduce ion flow to complete the electrical circuit are fragile, but as shown in Figure 9, have been engineered to be easier for the user to manipulate and operate.[106] Glycan structure can be elucidated from electrospray ionization without fragmentation by employing mass deconvolution,[98] a combination of exoglycosidases and exact mass.[91,103] However, several groups have demonstrated the value of fragmentation with electrospray ionization for identifying *N*-glycan structure.[104,105]

DOI: 10.1021/acs.chemrev.7b00669
Chem. Rev. 2018, 118, 7867−7885

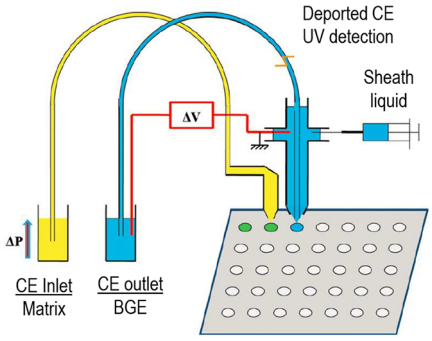

Figure 8. An instrument setup for off-line coupling of capillary electrophoresis and matrix assisted laser desorption ionization mass spectrometry (MALDI-MS). The capillary electrophoresis instrument was modified to incorporate the automatic spotting device to deposit the capillary eluent to the MALDI plate from the outlet vial of the capillary electrophoresis instrument, and the matrix required for MALDI detection was delivered from the inlet vial. From ref 101. Copyright 2014 by John Wiley Sons, Inc. Reprinted by permission of John Wiley & Sons, Inc.

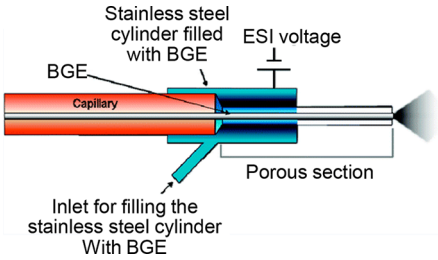

Figure 9. A cross sectional view of a sheathless CE-ESI MS interface including a porous tip in the front of the capillary outlet immersed in the background electrolyte (BGE) inside the stainless steel cylinder. Reprinted with permission from ref 106. Copyright 2010 American Chemical Society.

A recent report based on a previous microfluidic study[100] employed CE-MS electrospray ionization to reveal *N*-glycan structures in serum samples using a combination of chemical modification and fragmentation.[104] In this paper, the microfluidic laser-induced fluorescence technique provided better separation efficiency than the CE-MS; however, the advantage of using the CE-MS method is that the information from intact and fragment mass (m/z) enables the distinction of branched *N*-glycans, which could not be identified based on the migration time of the standards alone due to comigration, as shown in Figure 10. The sialylated (α2−6 and α2−3 linkages) *N*-glycans were derivatized with 4-(4,6-dimethoxy-1,3,5-triazin-2-yl)-4-methyl-morpholinium chloride following the production of amidated α2−6 linkages and lactones from α2−3 linkages. As a result, α2−3 and α2−6 linkages were distinguished from one another based on differences in mass as well as the electrophoretic mobilities. Cross-ring fragmentations generated from high energy collision induced dissociation further enabled the technique to identify linkage and positional isomers. As a result, 31 new *N*-glycan structures were recognized with a total of 77 structures identified from serum samples, which was an improvement over the previous study which identified a total of 37 *N*-glycan structures.[100]

Tandem mass tag, an isobaric tag, was designed to utilize fragment ions derived from tandem mass spectrometry for quantitative analysis of peptides and proteins, as well as *N*-glycans.[105,107,108] Tandem mass tags are composed of the mass

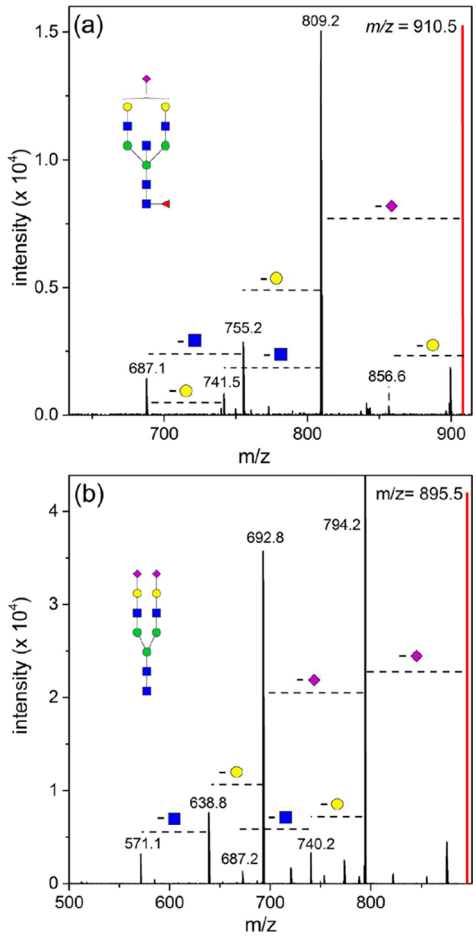

Figure 10. MS/MS spectrum of two glycans that overlapped in the capillary electrophoresis separation. The red line in the spectrum shows the signal (m/z) of the precursor ions selected for MS^2 scan. The observed Y-type fragment ions in the MS/MS spectrum indicate the identity of the monosaccharide that is lost. Reprinted from ref 104, Copyright 2017, with permission from Elsevier.

reporter, mass normalizer, and reactive functional groups.[108] The reactive functional groups (hydrazide or aminooxy moieties) are attached to the reducing end of the *N*-glycans through reductive amination. Both the mass reporter and mass normalizer groups contain isotope elements (^{13}C, D, or ^{15}N), so that the total mass of the tandem mass tag between the multiplexed labeling remains the same. Mass reporter ions are generated by collision-induced dissociation along with *N*-glycan fragments, and the relative abundance of each *N*-glycan is derived from the integrated area in extracted ion electropherograms. The use of aminooxy tandem mass tag labeling for *N*-glycan analysis was performed using CE electrospray ionization MS. Additionally, traveling wave ion mobility was incorporated after collision-induced dissociation as a second-dimension separation based on gas-phase mobilities. This was utilized to determine the relative abundance of *N*-glycan isomers through improved resolution. To generate a high abundance of reporter ions in the collision-induced dissociation cell, a pseudo-MS^3 method was applied.[105] Instead of using collision-induced dissociation results (i.e., MS^2 scan), both the intact *N*-glycan and *N*-glycan fragments that contain tandem mass tag reporter ions are observed, as shown in Figure 11. The Y1 fragment (m/z = 523), which is composed of monosaccharide and tandem mass tag, was generated in the ion source by increasing the

DOI: 10.1021/acs.chemrev.7b00669
Chem. Rev. 2018, 118, 7867−7885

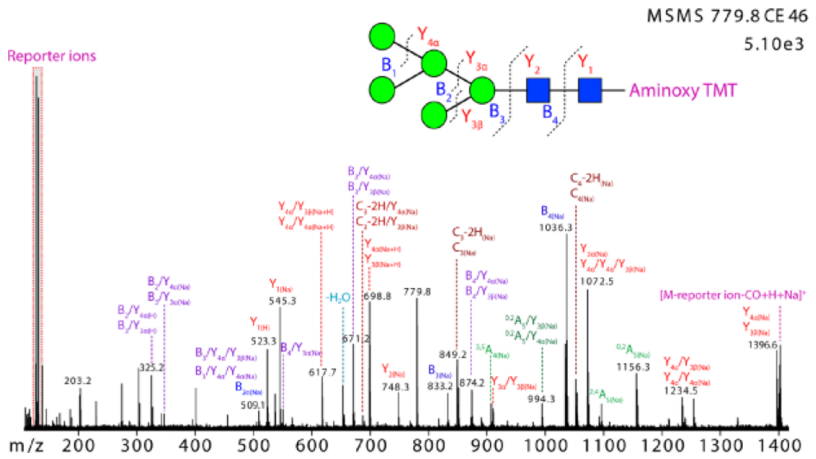

Figure 11. A representative MS/MS spectrum of a tandem mass tag (TMT) labeled glycan (m/z 779.8). The fragmentation of the TMT labeled glycan is depicted in the structure above the spectrum. The reporter ions, used for quantification, are observed in the lower mass range of the spectrum. Reprinted with permission from ref 105. Copyright 2015 American Chemical Society.

cone voltage from 30 to 100 V. Once Y1 fragments were selected as the precursor ions, the mass spectra obtained from the MS^2 scan reveals reporter ions in the absence of interferences from *N*-glycan fragment ions. This is beneficial as the *N*-glycan fragments generally dominate the tandem mass spectra and make it difficult to detect the reporter ion. The quantification of *N*-glycans, including both high mannose and complex types, was demonstrated using the integrated areas of the reporter ions in the MS^2 scan generated from $[M + Na + H]^{2+}$, $[M + 2H]^{2+}$, and $[M + 2H + K]^{3+}$ precursor ions.

5. APPLICATIONS

As described in this review, CE is a separation-based assay to identify and quantify carbohydrates. Generally, the method is adopted to address barriers in measurement technologies and then translated into a routine technique for monitoring industrial or clinical processes. Several areas of high activity were noted from 2014 to 2017 and are reviewed here. Glycans were heavily studied during this review period and a strong emphasis was apparent in biomarker discovery and biotherapeutic monitoring. This activity can be attributed to the separation power of CE and the ability to resolve complex mixtures and to separate positional isomers based on subtle differences in hydrodynamic volume. This has a profound impact on biological therapeutics where glycosylation is linked to product quality. Other areas, which are less prominent but also warrant attention, include characterization of glycosaminoglycans, as well as analyses of carbohydrates in food and plants.

5.1. Biomarkers

5.1.1. Changes within and across Individuals. The value of glycans as biomarkers has been established[109] in the past 5 years and continues to advance steadily. The variability associated with glycosylation as it occurs in the body must be assessed to establish the value in monitoring glycosylation as a biomarker for diseases. Hennig et al. noted a strong need to evaluate the stability of *N*-glycan profiles because most biomarker studies involve measurements at a single time point across disease states.[88] The purpose of the work by Hennig was to extend a prior study of individual variability within a 1-week period[110] and to build on prior reports that glycosylation is impacted by genetic background[111] or age.[112] The study by Hennig et al. utilized plasma samples from five healthy male volunteers over periods ranging from 1.5 to 6 years resulting in 135 samples.[88] Sampling intervals were more frequent during the first year. Lifestyle and health were noted 2 days prior to blood sampling and correlated with changes in the glycosylation profile. Plasma volumes of only 2 μL were used to obtain *N*-glycans that were separated using capillary gel electrophoresis and an instrument with 16 capillaries in parallel. The *N*-glycan composition was characterized with the aid of off-line exoglycosidase digestion (α2−3 and α2−3,6,8 sialidase; α1−3,4 and α1−2,3,4,6 fucosidase; β1−4 galactosidase; α1−2,3,6 mannosidase; 1−2,3,4,6 *N*-acetyl glucosaminidase) of *N*-glycans to identify the structure of the 31 most abundant sialylated and asialylated peaks. The *N*-glycan assignment for each sample was assessed using a DNA internal standard with glyXtool for assignment by *N*-glycan migration time in the database, and the relative peak height proportions were calculated to transform migration data into an *N*-glycan fingerprint. The reproducibility of the method was determined across many variables and the average variability in the relative peak height proportions were 5.4% RSD in overall (n = 10) measurements with greater variability observed in low abundance peaks (11%) than for medium to high abundance (3%). Except in cases of illness or injury, the variation within an individual was low throughout the time course of the study but was higher across individuals. Injury evoked an increase in sialylated *N*-glycans and a marginal increase in galactosylation. Illness, associated with allergic response, led to an increase in the amount of triantennary *N*-glycan accompanied by a decrease in biantennary *N*-glycan composition. The authors concluded that *N*-glycan biomarkers may be well suited as personalized biomarkers, with changes in glycosylation monitored in an individual routinely prior to illness.[88]

5.1.2. Autoimmune Disorders. Glycosylation is strongly linked to autoimmune disorders, and it has been postulated that unique *N*-glycan signatures associated with specific motifs at a specific antibody glycosylation site serve to identify and distinguish different autoimmune conditions.[113] Current research focuses on changes in antibody glycosylation as a means to provide insight into disease progression. Huang et al. used a combination of matrix assisted laser desorption ionization time-of-flight MS for structural confirmation and CE for identification and quantification of *N*-glycan isomers

DOI: 10.1021/acs.chemrev.7b00669
Chem. Rev. 2018, 118, 7867−7885

associated with rheumatoid arthritis (n = 15 patients against n = 15 controls).[55] CE results centered on 11 *N*-glycans, which demonstrated a decrease relative to healthy controls (p = 0.0001) in the galactosylation index, which is defined as the fractional composition of galactosylated *N*-glycan to total *N*-glycan response.[55] In a separate study, CE was used to evaluate the responsiveness of IgG treatment for both rheumatoid arthritis and Crohn's disease to treatment with anti-TNFα.[67] The *N*-glycan was derived from IgG isolated in serum samples that were collected 2 weeks post-treatment. For rheumatoid arthritis patients (n = 17), responding to the treatment (n = 11) was associated with changes only in 3 low abundance structures. Crohn's disease patients responding to treatment (n = 14) exhibited changes in several low abundant and a single high abundant *N*-glycan. One candidate biomarker from the low abundance *N*-glycans was statistically significant (p = 0.01).

CE was also used in conjunction with matrix assisted laser desorption ionization time-of-flight MS to profile HIV envelope glycoprotein. Guttman et al. analyzed the *N*-glycan composition of the gp120 subunit of the HIV envelope glycoprotein.[59] This subunit is of interest because it is highly (50% by mass) glycosylated. These researchers were able to demonstrate similarities among 3 recombinant gp120 samples (CM244, mother and infant) and then differences with a fourth sample (A244). Structural identification was possible using matrix assisted laser desorption ionization time-of-flight MS and a host of benchtop exoglycosidase reactions coupled with CE separations. A maltooligosaccharide ladder was used for peak assignment across runs.

5.1.3. Cancer. Excellent reviews have been published on the relevance of glycosylation to cancer diagnosis and prognosis.[114] Glycoconjugates are implicated in proliferation of malignant cells, migration, adhesion, and tumor evasion of the immune system. A hallmark of cancer is a change in the glycosylation pattern in tumor tissue and serum.[109,115,116] Mannose branching,[117] increased *N*-acetylglucosamine branching,[9] bisecting *N*-acetylglucosamine,[9] change in fucosylation[9,118] or polylactosamine,[9,119] and increase in sialic acid content.[9,109] Most work involves *N*-glycans derived from glycoproteins; although a few analyses of intact glycoproteins have been reported.[120,121] Several glycosylation signatures are associated with many different types of cancer.[109]

CE has recently been used to analyze *N*-glycans derived from IgG in serum as a method for diagnosing epithelial ovarian cancer.[62] Schwedler et al. identified *N*-glycans using a standard library derived from glycoproteins subject to exoglycosidase (benchtop) digestion and migration times evaluated with the use of a GU migration time calibration. Through this effort 32 *N*-glycans were identified. When applied to a patient cohort of stage 3 or 4 epithelial ovarian cancer (n = 10) and healthy individuals (n = 5), researchers found significant differences in increased *N*-glycan branching and fucosylation in the samples from cancer patients. In a separate report, this research cohort focused on changes in glycosylation attributed to acute phase proteins to identify protein-specific differences in glycosylation for epithelial ovarian cancer.[121] Proteins extracted using isoelectric focusing and two-dimensional slab gels were identified with matrix assisted laser desorption ionization time-of-flight MS and subsequently extracted, in order to analyze the *N*-glycans by CE. With a small patient cohort (n = 5 cancer, n = 5 controls), several differences were identified among 7 acute phase proteins.

The sialylated *N*-glycans from ovarian cancer patients were investigated using methylation of sialic acids to enhance the separation.[61] The benefit of modifying sialic acid residues, for example, with methylation, is that chemical modification eliminates the charge. The increased mass of each modified residue leads to differences in mobility observed as slower migration times. This improves the peak resolution relative to traditional CE approaches. Sialylated *N*-glycans derived from IgG in serum were separated using a labeled glycan ladder and quantified. Using the methylation strategy, researchers were able to successfully resolve biantennary *N*-glycan from monosialylated, fucosylated biantennary *N*-glycan, which enabled them to observe a significant increase in biantennary *N*-glycan in epithelial ovarian cancer patients (n = 5) relative to the controls. A comparison of the results obtained for other *N*-glycans were similar with or without the methylation approach.

Sialic acids containing *N*-glycans have been chemically modified via methylamidation to enhance peak resolution, and the electrophoretic separations were capable of resolving *N*-glycans with different linkage positions.[100] In a separate study, chemical modification of sialic acid residues was also utilized in conjunction with microchip electrophoresis to identify biomarkers in colon cancer.[99] Modification of sialic acid residues led to a predictable change in the charge-to-size ratio of *N*-glycans and allowed for a better distribution of the *N*-glycans throughout the electrophoretic separation window. Differences in glycosylation among healthy controls (n = 20) and patients with colorectal cancer were evaluated following the first chemotherapy treatment (n = 26) and the third chemotherapy treatment (n = 16). The microchip electrophoresis yielded exceptional migration reproducibility (0.03% RSD), efficiency (700 000 theoretical plates), and separation speed (135 s). Matrix assisted laser desorption ionization time-of-flight MS and electrophoresis were used as complementary analytical tools, and both methods identified the same *N*-glycans as potential biomarkers to distinguish healthy controls from cancer patients following different treatment time points. These changes in the glycosylation profile were observed between treatments, demonstrating the potential to use glycosylation profiles to stage colorectal cancer.

CE was used to identify two fucosylated *N*-glycans to distinguish light chain multiple myeloma from IgG myeloma from IgA myeloma using a set of 12 *N*-glycans collected from 2 μL of serum from each patient.[52] The relative abundance of each peak was used for statistical comparison and was calculated as the sum of each peak to the cumulative peak area. In total, 167 samples were assessed from patients with light chain multiple myeloma (n = 42), IgG myeloma (n = 42), IgA myeloma (n = 41), and healthy controls (n = 42). In a separate study,[92] the same group evaluated *N*-glycans in serum from a patient cohort with gastric cancer (n = 25) and gastric ulcer (n = 80) as compared to healthy controls (n = 139). The study focused on fucosylation; 7 of the 9 *N*-glycans identified in the set were fucosylated. While specific fucosylated *N*-glycans decreased or increased, the total abundance of fucosylation reportedly decreased in gastric ulcer and in gastric cancer. Other researchers also determined that differences in fucosylated *N*-glycans in urine, as well as differences in triantennary structures, are potential biomarkers that complement prostate specific antigen in order to better differentiate patients with prostate cancer (n = 42) from those with benign prostrate hyperplasia (n = 62).[68]

DOI: 10.1021/acs.chemrev.7b00669
Chem. Rev. 2018, 118, 7867−7885

5.1.4. Biomarker Studies of Cells. Others have also worked to expand the role of glycosylation in development, cellular differentiation, and aging. For instance, placental *N*-glycans have been profiled in an effort to obtain baseline data about glycosylation changes associated with the age of the mother or the period of gestation.[122] Both tissues cultured from animals and immortalized cells derived from tissue can be used to evaluate disease and the efficacy of treatment; however fundamental questions remain about the suitability of these systems. Complex *N*-glycans and glycosaminoglycans were monitored to provide insight into differences across an *in vitro* and *in vivo* model.[76] Both *N*-glycans and glycosaminoglycans were isolated and labeled, although the glycosaminoglycans were first digested with Pronase then chondroitinase. When analyzed by CE, carbohydrate profiles were different in cornea tissue as compared to immortalized cornea cells (i.e., Statens Seruminstitut rabbit cornea cells). The reason for these differences in *N*-glycan and glycosaminoglycan profiles was attributed to transition from epithelial to mesenchymal cells, warranting caution when comparing results across the tissue and immortalized cells derived from cornea tissue.

Other approaches centered on models of cell differentiation. Thiesler et al. used CE in conjunction with several biochemical assays to demonstrate a change in the *N*-glycan profile in cultured cells used to model different stages of PMM2-congenital disorder of glycosylation, a rare inherited disease.[66] These researchers focused on changes observed in high mannose *N*-glycans in cells used to model cells from healthy individuals as compared to phosphomannomutase 2-induced pluripotent stem cells developed to model the disorder. Many biochemical methods were utilized to complement the CE. CE separations of 22 *N*-glycans were transformed into fingerprints using *N*-glycan standards derived from asialofetuin.[66] Six abundant high-mannose-type *N*-glycans decreased in the phosphomannomutase 2-induced pluripotent stem cells.[66] In a separate study, changes in glycosylation were monitored during cellular differentiation of human induced pluripotent stem cells into cardiomyocytes using CE as well as MS.[123] Migration time precision and normalization of peak area were accomplished with an internal standard and GlyXtool software. Ten *N*-glycans changed across three time points (day 0, 7, and 15)[123] and supported the findings of previous studies of cardiomyocyte differentiation. In addition, three unique *N*-glycans previously not reported in these systems were found to decrease after the initial (day 0) measurement.[123]

5.2. Application to Biological Therapeutics

Sialylation on intact glycoproteins or glycopeptides is detected by CE because the negative charge changes the charge-to-size ratio and affects the mobility. This was demonstrated for a biological glycoprotein manufactured by Amgen.[124] Proteins were isolated using an isoelectric focusing separation prior to CE with UV−visible absorbance detection. Using an acidic background electrolyte, capillary coated with poly(vinyl alcohol), and reversed polarity, the product was separated into 9 peaks of different sialic acid composition. The sialic acid content was verified using a standard ninhydrin assay. Mapping of *N*-glycans was accomplished by enzymatically releasing *N*-glycans, which were then analyzed using MS. The separation could be used to evaluate protein products from different cell clones, to monitor the optimization of the preparative scale purification of the therapeutic product, and finally to monitor the product stability.

CE coupled with UV−visible absorbance detection or electrospray ionization and MS were used to compare the antibody-based drug cetuximab to a proposed generic replacement.[98] Cetuximab contains glycosylation sites in the antibody hinge region and near the Fab binding region. The glycosylation at these sites was distinguished using immunoglobulin degrading enzyme to cleave the intact $F(ab)_2$ region from the Fc chain. The protein fragments were separated and analyzed using a background electrolyte compatible with the sheathless electrospray ionization-MS and a capillary covalently modified with hydroxypropylcellulose to suppress EOF. The Fc2 fragment was resolved into multiple peaks, which contained 2 terminal lysine variants and different glycosylation. The $F(ab)_2$ fragments were separated into multiple peaks each containing different *N*-glycans. Four different sialylated *N*-glycan structures on some of the fragments were identified because sialylated *N*-glycans cause both a mobility shift and mass shift detectable by CE coupled to MS.

CE coupled with sheathless electrospray ionization and MS was also used to quantitatively characterize Avonex, which is a recombinant interferon-β1.[91] The protein was separated using a covalently cross-linked polyethyleneamine capillary and an acidic background electrolyte under conditions of reversed polarity. Of the 138 proteoforms, 55 were analyzed for deamidation, methionine loss, and glycosylation. The high efficiency of the separation resolved isobaric positional isomers of sialic acid residues and polyLacNac. Bench top reactions with exoglycosidases (galactosidase or sialidase) were conducted to confirm these structures.

Gahoual et al. utilized CE coupled with sheathless electrospray to compare two patented therapeutics with generic alternatives, called biosimilars.[125] CE was used to analyze glycopeptides from trastuzumab, cetuximab, and the biosimilar candidates to establish glycosylation. Cetuximab has two sites of glycosylation, and analysis of peptide fragments from the Fd domain within the antigen binding region established that the generic substitute did not contain α1−3 galactose residues found in the innovator drug. This is important because α-galactose is a non-human structure that elicits an adverse immune response. A generic form of cetuximab lacking α-galactose is a better product than the original drug, potentially making the generic form a new drug that can be patented.

A microchip electrophoresis separation with integrated nanoelectrospray ionization was coupled to MS to characterize several features of an antibody−drug conjugate.[126] The approach demonstrated the ability to confirm the presence of different glycosylation on the antibody. In a separate report, the same chip-based nanoelectrospray system was used to assess glycation on hemoglobin as a potential biomarker for diabetes management.[127]

5.3. Other Carbohydrates

5.3.1. Glycosaminoglycans. Several reports have appeared during the time frame of this review on glycosaminoglycans, which are linear polymers that contain repeating disaccharide units of uronic acid and hexosamine residues. The most widely discussed glycosaminoglycan is heparin. Heparin is used as an anticoagulant, and monitoring the quality of heparin prior to administering it to patients has become particularly important after the deaths of over 100 people, which were attributed to the contamination of pharmaceutical heparin.[128,129]

Heparin is one of the most structurally complex glycosaminoglycans. Heparin has variable degrees of sulfation

DOI: 10.1021/acs.chemrev.7b00669
Chem. Rev. 2018, 118, 7867−7885

and alternating repeating units of α1−4 linked residues of L-iduronic acid and *N*-,*O*-disulfated glucosamine, as shown in Figure 12. The R groups represent where the structure can be

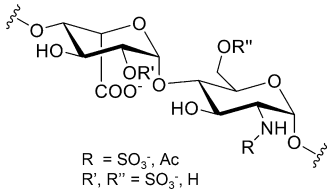

Figure 12. Schematic of heparin disaccharide. The repeating disaccharide is composed of L-iduronic acid and D-glucosamine joined by an α1−4 glycosidic linkage. The R group can be either sulfate or acetate and R′ and R″ can be either sulfate or hydrogen.

substituted with a sulfate, hydrogen, or acetate group. There are eight possible combinations for heparin disaccharides depending upon the substituent group. The sheer heterogeneity of glycosaminoglycan structures presents an analytical challenge that is addressed through analyses of disaccharide composition. Analysis of even small glycosaminoglycan fragments is a daunting task and separation-based methods are still evolving.[128,129] In an effort to address that need, a CE-MS method providing label-free, rapid, and sensitive analysis to characterize sulfated disaccharides and low molecular weight heparins was developed employing both positive[130] and negative modes.[131] An electrokinetic pump-based interface was used to couple the CE separation to the analysis. Different degrees of sulfation on the disaccharide were separated due to variation in the carried charges, and the identity was verified by exact mass. Both bottom-up and top-down approaches were applied to reveal the various sulfated disaccharides in Lovenox, a polycomponent low molecular weight heparin used for anticoagulant treatment. Sulfated disaccharide structures in relatively low abundance were identified with this method as a result of the 1000-fold enhancement in the limit of detection when the mass spectrometer was utilized as compared to UV detection. Twenty different types of low molecular weight heparins were identified with different characteristics with respect to sulfate, acetate, and 1,6 anhydrate groups.[130]

CE methods were also developed to profile and quantify other glycosaminoglycans, including heparan sulfate,[132,133] chondroitin sulfate,[132−134] dermatan sulfate,[133,134] hyaluronan,[134] and keratin sulfate.[133] Glycosaminoglycans are typically first depolymerized using glycosaminoglycan lyases,[132,133] which form disaccharides that are fluorescently labeled and separated based on the number of charged groups. One method achieved rapid profiling of up to 19 disaccharides in a single run.[133] CE techniques for profiling these glycosaminoglycans in urine have been demonstrated and hold the potential to be utilized for diagnosis of diseases in newborns, since uronic acid glycosaminoglycans serve as biomarkers for various diseases.[132] While depolymerization of glycosaminoglycans is commonly performed, other studies demonstrate the use of CE for the analysis of intact heparin, chondroitin sulfate, dermatan sulfate, and hyaluronan,[134] as well as K4 and K5 capsular polysaccharides that are chondroitin sulfate and heparin starting materials.[135]

In addition to monitoring glycosaminoglycans in samples, CE has also been applied to study the binding interactions of glycosaminoglycans with apolipoproteins.[136] Witos et al. utilized a partial filling-affinity CE technique in order to distinguish weak and strong binding between glycosaminoglycans and apolipoproteins. An excellent discussion of the power of CE, including different modes of separation, to elicit information about glycosaminoglycans and proteins in general has recently been published.[137]

5.3.2. Food and Plant Carbohydrate Analyses. Carbohydrates relevant to food and plants pose several challenges for analysis that have resulted in the development of strategic techniques to overcome these barriers. These carbohydrates are neutral and do not absorb well in the UV range, which makes analysis using CE combined with UV detection difficult. To facilitate the CE separation, mono- and disaccharides are commonly separated by employing a borate buffer, as has been demonstrated recently using samples such as caprine milk,[138] honey,[139] and the herb purslane.[140] Boric acid forms negatively charged complexes with diol groups, which circumvents the issue of the carbohydrates being neutral and enables the separation of the mono- and disaccharides by charge-to-size ratio. These mono- and disaccharides can also be separated by adjusting the pH of the background electrolyte to a pH above 11. Using these extremely alkaline buffers causes deprotonation of the carbohydrates and provides a negative charge. The technique has been applied for the charge-to-size ratio separation of mono- and disaccharides in a wide variety of food and plants, such as honey,[141] breakfast cereals,[142] juice and nectar from fruits,[143] and others.[144−146] While most of these analyses rely on direct[139,140,142,144] or indirect[138,141,143,145] detection by UV absorbance, one study demonstrated the use of capacitively coupled contactless conductivity detection coupled with electrospray ionization MS,[146] which the authors suggest can be used for the detection of neutral species that may be overlooked in electrospray ionization MS due to poor ionization efficiency.

More complex polysaccharides, such as amylopectin, found in food and plants are typically analyzed using fluorophore assisted carbohydrate electrophoresis.[45,147−150] For this technique, the polysaccharides are debranched using enzymes. The polysaccharide fragments produced by debranching each contain a reducing end to which a fluorophore can be conjugated. This enables detection of the debranched polysaccharides through laser-induced fluorescence. Debranching also reduces the structure down to the linear chain, removing the complication of changes in hydrodynamic volume due to the branches when determining the degree of polymerization. Once derivatized with a fluorophore, the carbohydrates are analyzed using a neutral coated capillary under reverse polarity. This technique had been utilized to quantify the polydispersity of amylopectin in food, a characteristic that impacts the quality of rice,[147] up to a degree of polymerization of 160.[148,150] While digestion is not necessary for the carbohydrate analysis,[45,147,148,150] one report demonstrates the applicability of this method to examine the ability for a starch to be digested in the body by analyzing carbohydrate profiles after performing an *in vitro* digestion.[149]

6. EMERGING TECHNIQUES AND FUTURE DIRECTIONS

6.1. High Throughput Structural Characterization of Biological Therapeutics

The establishment of CE in so many diverse applications is a testament to the importance of this method in glycosciences. Given the accelerating discoveries in glycosylation and the ever

DOI: 10.1021/acs.chemrev.7b00669
Chem. Rev. 2018, 118, 7867−7885

evolving need for new technologies, CE will play a more prominent role in this field. Certain aspects of this technology are areas to watch for future growth. The first area of profound impact will be as a tool to complement current[18,47,94,95] and emerging techniques[151] to characterize and quantify positional and linkage isomers for the exploding biological therapeutics market. Several collective innovations make this possible. Significant progress has been achieved for migration time databases using polysaccharide or DNA ladders that yield unprecedented precision in time-based peak identification for CE separations coupled with fluorescent detection. The sample preparation bottleneck is addressed with new tools for integrated and automated multistep processing. This streamlined work flow for sample preparation begins with raw sample and ends with injection-ready glycans by automating antibody purification, deglycosylation, labeling, and sample clean up. With the easy generation of large batches of samples, manufacturers of biologics have the power to easily and routinely monitor changes in glycosylation that can occur with change in the cell culture conditions.[10] This level of automated monitoring utilizing commercial robotics, as shown in Figure 13, will ultimately improve the quality of products delivered to consumers.

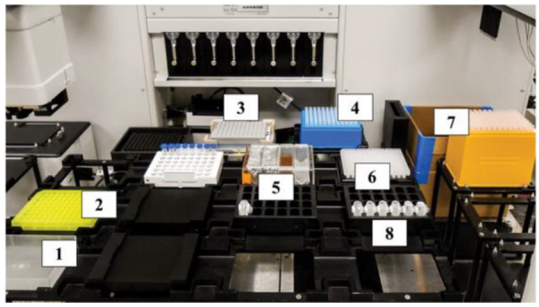

Figure 13. Photograph of the laboratory set up for the Biomek FXP Laboratory Automation Workstation, which was used to automate work flow for APTS labeling and purification of carbohydrates. The lab materials required for this include a lid for the pipet box to reduce evaporation (1), a 96-sample tray for a capillary electrophoresis instrument (2), a Peltier shaker (3), 20 μL pipet tips (4), labeling reagents and magnetic beads (5), a 96-well PCR plate on a magnetic stand (6), 1000 μL pipet tips (7), and a 24-well plate for large volumes of reagent (8). From ref 64. Copyright 2016 by SAGE Publications, Reprinted by Permission of SAGE Publications, Inc.

The use of lectins and enzymes has become more common, and commercial systems have been adapted to automatically incubate and process exoglycosidase reactions for improved linkage and monomer identification.[152] The high cost and long reaction times make integration of enzymatic processing less appealing but the potential of using in-line methods of enzyme processing are a promising solution.[96] The recent discovery of materials to increase the enzyme lifetime from days to months is fundamental to lowering the overall cost.[77,93] A dramatic reduction in cost and time is realized when nanoliter reaction volumes are used. Patterning separation capillaries with sequential enzyme cartridges is an effective step forward to higher throughput screening with enzymes and is also invaluable to screening for the potential for enzymatic remodeling of glycosylation.

6.2. Realizing the Full Power of Electrophoresis and MS

The benefit of more conclusive structural identification can be achieved if the strengths of MS and CE are leveraged. This is demonstrated in reports that utilize differences in mobilities to distinguish linkage position[102] or harness the MS to resolve peaks that comigrate[102,104] in CE. A second area of growth to watch is a growing use of commercial systems that couple CE and MS. The commercialization of robust interfaces for end-users has dramatically increased the accessibility of the method. These include the means to decouple the separation current from the electrospray process while avoiding dilution associated with the transfer of the nanoliter flow rates in the electrophoresis capillary.[106] Improvements in the compatibility of electrophoresis and MS, including new ionization strategies and more flexibility in combining detection modalities, will increase the prevalence of CE in biomarker discovery. Growth in MS citations in glycosciences have paralleled citation rates for biomarker discovery. The current emphasis on analyses of glycopeptides and glycoproteins with CE-MS systems as changes in both the glycosylation pattern as well as the location of glycosylation may be more powerful in biomarker specificity and sensitivity. Combining the unprecedented separation power of CE, a migration database, and structural determination would lead to a high level of certainty in identification utilizing methods capable of high throughput analyses.

A commercial microfluidic electrophoresis device designed for MS is available (see Figure 14). The microfluidic device has

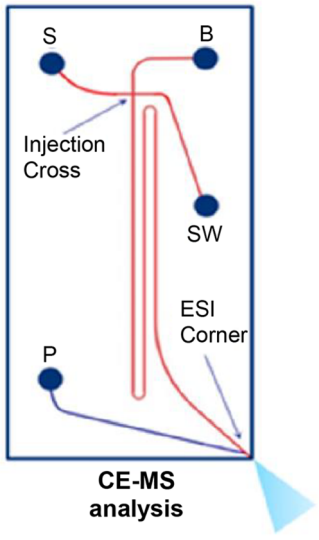

Figure 14. Schematic of a commercially available microfluidic chip for capillary electrophoresis–electrospray ionization–mass spectrometry. The chip consists of sample reservoir S, background electrolyte reservoir B, electrospray ionization pump P, and sample waste SW. The nanospray interface is integrated at the corner of the chip. Adapted with permission from ref 107. Copyright 2017 American Chemical Society.

been utilized for glycoprotein and glycopeptide analyses.[107,127,153] This recently developed microfluidic device (ZipChip CE), which is surface modified to minimize protein adsorption and suppress EOF, integrates the electrospray interface into the microfluidic chip maintaining steady flow rate and electrospray ionization. Mass spectrometric compatible buffers were employed for the separation of glycopro-

DOI: 10.1021/acs.chemrev.7b00669
Chem. Rev. 2018, 118, 7867–7885

teins,[126,127,153] glycopeptides,[107] oligosaccharides,[107] and monosaccharides.[107] The microfluidic devices have been utilized for separations of oligosaccharides and monosaccharides labeled with tandem mass tags, demonstrating the structural identification and quantification observed with high throughput and automated benchtop instruments.[107]

6.3. Future Directions

Researchers continue to tailor CE separations to meet the challenges faced by the carbohydrate chemistry community. As carbohydrate biomarkers gain more prominence, the technique will be adapted further. Future applications may rely on more portable methods of analyses based on microfluidic chips. These may utilize miniaturized detectors, contactless conductivity detection, or fluorescence detection with light emitting diodes and a CCD camera.[154] Finally, as new carbohydrates continue to be identified and as researchers strive to analyze highly complex mixtures, CE separations with higher peak capacity will gain more attention.

AUTHOR INFORMATION

Corresponding Author

*E-mail: Lisa.Holland@mail.wvu.edu.

ORCID

Lisa A. Holland: 0000-0002-7534-6810

Notes

The authors declare no competing financial interest.

Biographies

Grace (En-Tzu) Lu received both her B.S. and M.S. degrees in chemistry from National Taiwan University. Her research work focused on glycan analyses using CE coupled with MS. In 2012, she joined the research group of Prof. Amanda J. Haes at the University of Iowa, and in 2017, she completed her studies of CE analysis in enzymatic reactions and small molecule detection using surface-enhanced Raman scattering. She is currently a postdoctoral fellow in Professor Lisa A. Holland's research group at West Virginia University. Her research interests include developing analytical methods for glycan structure elucidation using CE.

Cassandra Crihfield received a B.S. degree in chemistry from Wheeling Jesuit University in 2013. Cassandra is a Ph.D. candidate in analytical chemistry at West Virginia University in the Holland group. She is a current interdisciplinary graduate education and research traineeship (IGERT) fellow and former NanoSAFE fellow. Cassandra's graduate research has focused on developing enabling techniques based on CE for the detection and characterization of small molecules, oligosaccharides, and proteins.

Srikanth Gattu has received his B.S. from Osmania University in 2009 and then completed his M.S. from Vellore Institute of Technology in 2011. He is currently a Ph.D. candidate in the research group of Prof. Lisa A Holland at West Virginia University. His research mainly focuses on integrating microscale enzyme reactions and lectin pulldowns using phospholipid assisted separations of biomolecules.

Lindsay Veltri is a senior undergraduate chemistry student at West Virginia University. She is the recipient of a 2017 ACS Division of Analytical Chemistry Undergraduate Award. Her academic interests include the design and application of microfluidic devices for medical diagnostics, drug discovery, and the development of nanomaterials for biological detection.

Lisa Holland received her B.S. degree in Chemistry from the University of Maryland at College Park, while working in the Electroanalytical Research Group at the National Institute of Standards and Technology. She received her Ph.D. in Chemistry from the University of North Carolina at Chapel Hill under the direction of Professor James Jorgenson. Through a National Research Service Award she held a postdoctoral fellowship under the direction of Professor Susan Lunte in the Department of Pharmaceutical Chemistry at the University of Kansas. Dr. Holland is the recipient of a National Science Foundation Faculty Early Career Development award, has numerous publications in the field of separation chemistry, and was elected to the position of executive board (2007−2012), Chair-Elect (2012−2015), and Chair (2015−2017) of the American Chemical Society Subdivision of Chromatography and Separation Chemistry. She holds a faculty position in the C. Eugene Bennett Department of Chemistry at West Virginia University, specializing in microscale separations of biomolecules relevant to human health. She enjoys teaching instrumental analysis to undergraduate and graduate students and mentoring the many outstanding researchers who have studied separation science at WVU.

ACKNOWLEDGMENTS

This material is based upon work supported by NIH Grant No. R01GM114330. C.L.C. acknowledges a National Science Foundation IGERT fellowship, DGE no. 1144676.

REFERENCES

(1) Pfrengle, F. Synthetic Plant Glycans. *Curr. Opin. Chem. Biol.* **2017**, *40*, 145−151.
(2) Shanker, S.; Hu, L.; Ramani, S.; Atmar, R. L.; Estes, M. K.; Venkataram Prasad, B. V. Structural Features of Glycan Recognition among Viral Pathogens. *Curr. Opin. Struct. Biol.* **2017**, *44*, 211−218.
(3) Kizuka, Y.; Kitazume, S.; Taniguchi, N. N-Glycan and Alzheimer's Disease. *Biochim. Biophys. Acta, Gen. Subj.* **2017**, *1861*, 2447−2454.
(4) Veillon, L.; Fakih, C.; Abou-El-Hassan, H.; Kobeissy, F.; Mechref, Y. Glycosylation Changes in Brain Cancer. *ACS Chem. Neurosci.* **2018**, *9*, 51−72.
(5) Miura, Y.; Endo, T. Glycomics and Glycoproteomics Focused on Aging and Age-Related Diseases — Glycans as a Potential Biomarker for Physiological Alterations. *Biochim. Biophys. Acta, Gen. Subj.* **2016**, *1860*, 1608−1614.
(6) de Oliveira, M. A. L.; Porto, B. L. S.; de A. Bastos, C.; Sabarense, C. M.; Vaz, F. A. S.; Neves, L. N. O.; Duarte, L. M.; da S. Campos, N.; Chellini, P. R.; da Silva, P. H. F.; et al. Analysis of Amino Acids, Proteins, Carbohydrates and Lipids in Food by Capillary Electromigration Methods: A Review. *Anal. Methods* **2016**, *8*, 3649−3680.
(7) Yu, X.; Marshall, M. J. E.; Cragg, M. S.; Crispin, M. Improving Antibody-Based Cancer Therapeutics through Glycan Engineering. *BioDrugs* **2017**, *31*, 151−166.
(8) Gabius, H.-J. The Sugar Code: Why Glycans Are So Important. *BioSystems* **2018**, *164*, 102−111.
(9) Kizuka, Y.; Taniguchi, N. Enzymes for N-Glycan Branching and Their Genetic and Nongenetic Regulation in Cancer. *Biomolecules* **2016**, *6* (1−21), 25.
(10) Batra, J.; Rathore, A. S. Glycosylation of Monoclonal Antibody Products: Current Status and Future Prospects. *Biotechnol. Prog.* **2016**, *32*, 1091−1102.
(11) Jefferis, R. Glyco-Engineering of Human IgG-Fc to Modulate Biologic Activities. *Curr. Pharm. Biotechnol.* **2016**, *17*, 1333−1347.
(12) Planinc, A.; Bones, J.; Dejaegher, B.; Van Antwerpen, P.; Delporte, C. Glycan Characterization of Biopharmaceuticals: Updates and Perspectives. *Anal. Chim. Acta* **2016**, *921*, 13−27.
(13) Beyer, B.; Schuster, M.; Jungbauer, A.; Lingg, N. Microheterogeneity of Recombinant Antibodies: Analytics and Functional Impact. *Biotechnol. J.* **2018**, *13* (1−11), 1700476.
(14) Mantovani, V.; Galeotti, F.; Maccari, F.; Volpi, N. Recent Advances in Capillary Electrophoresis Separation of Monosaccharides,

DOI: 10.1021/acs.chemrev.7b00669
Chem. Rev. 2018, 118, 7867−7885

Oligosaccharides, and Polysaccharides. *Electrophoresis* **2018**, *39*, 179−189.
(15) Mantovani, V.; Galeotti, F.; Maccari, F.; Volpi, N. Recent Advances on Separation and Characterization of Human Milk Oligosaccharides. *Electrophoresis* **2016**, *37*, 1514−1524.
(16) Hajba, L.; Csanky, E.; Guttman, A. Liquid Phase Separation Methods for N-Glycosylation Analysis of Glycoproteins of Biomedical and Biopharmaceutical Interest. A Critical Review. *Anal. Chim. Acta* **2016**, *943*, 8−16.
(17) Fekete, S.; Guillarme, D.; Sandra, P.; Sandra, K. Chromatographic, Electrophoretic, and Mass Spectrometric Methods for the Analytical Characterization of Protein Biopharmaceuticals. *Anal. Chem.* **2016**, *88*, 480−507.
(18) Gaunitz, S.; Nagy, G.; Pohl, N. L. B.; Novotny, M. V. Recent Advances in the Analysis of Complex Glycoproteins. *Anal. Chem.* **2017**, *89*, 389−413.
(19) Szekrényes, Á.; Park, S. S.; Santos, M.; Lew, C.; Jones, A.; Haxo, T.; Kimzey, M.; Pourkaveh, S.; Szabó, Z.; Sosic, Z.; et al. Multi-Site N-Glycan Mapping Study 1: Capillary Electrophoresis − Laser Induced Fluorescence. *mAbs* **2016**, *8*, 56−64.
(20) https://sciex.com/products/standards-and-reagents/fast-glycan-analysis-and-labeling-for-the-pa-800-plus, accessed November 01, 2017.
(21) https://www.thermofisher.com/order/catalog/product/A28676, accessed November 1, 2017.
(22) https://prozyme.com/products/gp24ng-apts, accessed November 01, 2017.
(23) https://www.ludger.com/products/glycan_labeling_kits.php, accessed February 17, 2018.
(24) www.waters.com/waters/en_CA/GlycoWorks-RapiFluor-MS-N-Glycan-Kit/nav.htm?locale=en_CA&cid=134828150, accessed February 17, 2018.
(25) Ecker, D. M.; Jones, S. D.; Levine, H. L. The Therapeutic Monoclonal Antibody Market. *mAbs* **2015**, *7*, 9−14.
(26) Jorgenson, J. W.; Lukacs, K. D. Capillary Zone Electrophoresis. *Science* **1983**, *222*, 266−272.
(27) Reusch, D.; Haberger, M.; Kailich, T.; Heidenreich, A.-K.; Kampe, M.; Bulau, P.; Wuhrer, M. High-Throughput Glycosylation Analysis of Therapeutic Immunoglobulin G by Capillary Gel Electrophoresis Using a DNA Analyzer. *mAbs* **2014**, *6*, 185−196.
(28) Feng, H.-t.; Lim, S.; Laserna, A. K. C.; Li, P.; Yin, X.; Simsek, E.; Khan, S. H.; Chen, S.-M.; Li, S. F. Y. High Throughput Human Plasma N-Glycan Analysis Using DNA Analyzer and Multivariate Analysis for Biomarker Discovery. *Anal. Chim. Acta* **2017**, *995*, 106−113.
(29) Mahan, A. E.; Tedesco, J.; Dionne, K.; Baruah, K.; Cheng, H. D.; De Jager, P. L.; Barouch, D. H.; Suscovich, T.; Ackerman, M.; Crispin, M.; Alter, G. A Method for High-Throughput, Sensitive Analysis of IgG Fc and Fab Glycosylation by Capillary Electrophoresis. *J. Immunol. Methods* **2015**, *417*, 34−44.
(30) Huffman, J. E.; Pučić-Baković, M.; Klarić, L.; Hennig, R.; Selman, M. H. J.; Vučković, F.; Novokmet, M.; Krištić, J.; Borowiak, M.; Muth, T.; et al. Comparative Performance of Four Methods for High-Throughput Glycosylation Analysis of Immunoglobulin G in Genetic and Epidemiological Research. *Mol. Cell. Proteomics* **2014**, *13*, 1598−1610.
(31) Feng, H.-t.; Li, P.; Rui, G.; Stray, J.; Khan, S.; Chen, S.-M.; Li, S. F. Y. Multiplexing N-Glycan Analysis by DNA Analyzer. *Electrophoresis* **2017**, *38*, 1788−1799.
(32) Kovács, Z.; Szarka, M.; Szigeti, M.; Guttman, A. Separation Window Dependent Multiple Injection (Swdmi) for Large Scale Analysis of Therapeutic Antibody N-Glycans. *J. Pharm. Biomed. Anal.* **2016**, *128*, 367−370.
(33) Stanley, P.; Schachter, H.; Taniguchi, N. In *Essentials of Glycobiology*, 2nd ed.; Varki, A., Cummings, R. D., Esko, J. D., et al., Eds.; Cold Spring Harbor Laboratory Press: Cold Spring Harbor (NY), 2009; Chapter 8. Available from: https://www.ncbi.nlm.nih.gov/books/NBK1917/.
(34) Shajahan, A.; Heiss, C.; Ishihara, M.; Azadi, P. Glycomic and Glycoproteomic Analysis of Glycoproteins—a Tutorial. *Anal. Bioanal. Chem.* **2017**, *409*, 4483−4505.
(35) Lindhorst Thisbe, K. *Essentials of Carbohydrate Chemistry and Biochemistry*; John Wiley Sons: Chichester, U.K., 2003.
(36) Holland, L. A.; Chetwyn, N. P.; Perkins, M. D.; Lunte, S. M. Capillary Electrophoresis in Pharmaceutical Analysis. *Pharm. Res.* **1997**, *14*, 372−387.
(37) Evangelista, R. A.; Liu, M.-S.; Chen, F.-T. A. Characterization of 9-Aminopyrene-1,4,6-Trisulfonate Derivatized Sugars by Capillary Electrophoresis with Laser-Induced Fluorescence Detection. *Anal. Chem.* **1995**, *67*, 2239−2245.
(38) Guttman, A. Analysis of Monosaccharide Composition by Capillary Electrophoresis. *J. Chromatogr. A* **1997**, *763*, 271−277.
(39) Szabo, Z.; Guttman, A.; Rejtar, T.; Karger, B. L. Improved Sample Preparation Method for Glycan Analysis of Glycoproteins by CE-LIF and CE-MS. *Electrophoresis* **2010**, *31*, 1389−1395.
(40) Váradi, C.; Lew, C.; Guttman, A. Rapid Magnetic Bead Based Sample Preparation for Automated and High Throughput N-Glycan Analysis of Therapeutic Antibodies. *Anal. Chem.* **2014**, *86*, 5682−5687.
(41) Oda, R. P.; Landers, J. P. In *Handbook of Capillary Electrophoresis*, 2nd ed.; Landers, J. P., Ed.; CRC Press: Boca Raton, FL, 1997; Chapter 1.
(42) Guttman, A.; Cooke, N.; Starr, C. M. Capillary Electrophoresis Separation of Oligosaccharides: I. Effect of Operational Variables. *Electrophoresis* **1994**, *15*, 1518−1522.
(43) Barnes, J.; Tian, L.; Loftis, J.; Hiznay, J.; Comhair, S.; Lauer, M.; Dweik, R. Isolation and Analysis of Sugar Nucleotides Using Solid Phase Extraction and Fluorophore Assisted Carbohydrate Electrophoresis. *MethodsX* **2016**, *3*, 251−260.
(44) Karousou, E.; Asimakopoulou, A.; Monti, L.; Zafeiropoulou, V.; Afratis, N.; Gartaganis, P.; Rossi, A.; Passi, A.; Karamanos, N. K. Face Analysis as a Fast and Reliable Methodology to Monitor the Sulfation and Total Amount of Chondroitin Sulfate in Biological Samples of Clinical Importance. *Molecules* **2014**, *19*, 7959−7980.
(45) Kuang, Q.; Xu, J.; Wang, K.; Zhou, S.; Liu, X. Structure and Digestion of Hybrid Indica Rice Starch and Its Biosynthesis. *Int. J. Biol. Macromol.* **2016**, *93*, 402−407.
(46) Vreeker, G.; Wuhrer, M. Reversed-Phase Separation Methods for Glycan Analysis. *Anal. Bioanal. Chem.* **2017**, *409*, 359−378.
(47) Hofmann, J.; Pagel, K. Glycan Analysis by Ion Mobility−Mass Spectrometry. *Angew. Chem., Int. Ed.* **2017**, *56*, 8342−8349.
(48) Geissner, A.; Seeberger, P. H. Glycan Arrays: From Basic Biochemical Research to Bioanalytical and Biomedical Applications. *Annu. Rev. Anal. Chem.* **2016**, *9*, 223−247.
(49) Reusch, D.; Haberger, M.; Maier, B.; Maier, M.; Kloseck, R.; Zimmermann, B.; Hook, M.; Szabo, Z.; Tep, S.; Wegstein, J.; Alt, N.; Bulau, P.; Wuhrer, M. Comparison of Methods for the Analysis of Therapeutic Immunoglobulin G Fc-Glycosylation Profiles-Part 1: Separation-Based Methods. *mAbs* **2015**, *7*, 167−179.
(50) Adamczyk, B.; Tharmalingam-Jaikaran, T.; Schomberg, M.; Szekrényes, Á.; Kelly, R. M.; Karlsson, N. G.; Guttman, A.; Rudd, P. M. Comparison of Separation Techniques for the Elucidation of IgG N-Glycans Pooled from Healthy Mammalian Species. *Carbohydr. Res.* **2014**, *389*, 174−185.
(51) Danyluk, H. J.; Shum, L. K.; Zandberg, W. F. In *Protein-Carbohydrate Interactions: Methods and Protocols*; Abbott, D. W., Lammerts van Bueren, A., Eds.; Humana Press: New York, NY, 2017, *1588*, 223−236.
(52) Chen, J.; Fang, M.; Zhao, Y.-P.; Yi, C.-H.; Ji, J.; Cheng, C.; Wang, M.-M.; Gu, X.; Sun, Q.-S.; Chen, X.-L.; Gao, C.-F. Serum N-Glycans: A New Diagnostic Biomarker for Light Chain Multiple Myeloma. *PLoS One* **2015**, *10*, No. e0127022.
(53) Donczo, B.; Szigeti, M.; Ostoros, G.; Gacs, A.; Tovari, J.; Guttman, A. N-Glycosylation Analysis of Formalin Fixed Paraffin Embedded Samples by Capillary Electrophoresis. *Electrophoresis* **2016**, *37*, 2292−2296.

DOI: 10.1021/acs.chemrev.7b00669
Chem. Rev. 2018, 118, 7867−7885

(54) Guttman, A.; Kerekgyarto, M.; Jarvas, G. Effect of Separation Temperature on Structure Specific Glycan Migration in Capillary Electrophoresis. *Anal. Chem.* **2015**, *87*, 11630−11634.
(55) Huang, C.; Liu, Y.; Wu, H.; Sun, D.; Li, Y. Characterization of IgG Glycosylation in Rheumatoid Arthritis Patients by MALDI-TOF-MS^n and Capillary Electrophoresis. *Anal. Bioanal. Chem.* **2017**, *409*, 3731−3739.
(56) Jarvas, G.; Szigeti, M.; Guttman, A. GUcal: An Integrated Application for Capillary Electrophoresis Based Glycan Analysis. *Electrophoresis* **2015**, *36*, 3094−3096.
(57) Kovács, Z.; Papp, G.; Horváth, H.; Joó, F.; Guttman, A. A Novel Carbohydrate Labeling Method Utilizing Transfer Hydrogenation-Mediated Reductive Amination. *J. Pharm. Biomed. Anal.* **2017**, *142*, 324−327.
(58) Donczo, B.; Szarka, M.; Tovari, J.; Ostoros, G.; Csanky, E.; Guttman, A. Molecular Glycopathology by Capillary Electrophoresis: Analysis of the N-Glycome of Formalin-Fixed Paraffin-Embedded Mouse Tissue Samples. *Electrophoresis* **2017**, *38*, 1602−1608.
(59) Guttman, M.; Váradi, C.; Lee, K. K.; Guttman, A. Comparative Glycoprofiling of Hiv Gp120 Immunogens by Capillary Electrophoresis and MALDI Mass Spectrometry. *Electrophoresis* **2015**, *36*, 1305−1313.
(60) Meininger, M.; Stepath, M.; Hennig, R.; Cajic, S.; Rapp, E.; Rotering, H.; Wolff, M. W.; Reichl, U. Sialic Acid-Specific Affinity Chromatography for the Separation of Erythropoietin Glycoforms Using Serotonin as a Ligand. *J. Chromatogr. B: Anal. Technol. Biomed. Life Sci.* **2016**, *1012*, 193−203.
(61) Schwedler, C.; Kaup, M.; Petzold, D.; Hoppe, B.; Braicu, E. I.; Sehouli, J.; Ehlers, M.; Berger, M.; Tauber, R.; Blanchard, V. Sialic Acid Methylation Refines Capillary Electrophoresis Laser-Induced Fluorescence Analyses of Immunoglobulin G N-Glycans of Ovarian Cancer Patients. *Electrophoresis* **2014**, *35*, 1025−1031.
(62) Schwedler, C.; Kaup, M.; Weiz, S.; Hoppe, M.; Braicu, E. I.; Sehouli, J.; Hoppe, B.; Tauber, R.; Berger, M.; Blanchard, V. Identification of 34 N-Glycan Isomers in Human Serum by Capillary Electrophoresis Coupled with Laser-Induced Fluorescence Allows Improving Glycan Biomarker Discovery. *Anal. Bioanal. Chem.* **2014**, *406*, 7185−7193.
(63) Szekrényes, Á.; Partyka, J.; Varadi, C.; Krenkova, J.; Foret, F.; Guttman, A.In *Microchip Capillary Electrophoresis Protocols*; Van Schepdael, A., Ed.; Humana Press: New York, NY, 2015, *1274*, 183−195.
(64) Szigeti, M.; Lew, C.; Roby, K.; Guttman, A. Fully Automated Sample Preparation for Ultrafast N-Glycosylation Analysis of Antibody Therapeutics. *J. Lab. Autom.* **2016**, *21*, 281−286.
(65) Szigeti, M.; Bondar, J.; Gjerde, D.; Keresztessy, Z.; Szekrenyes, A.; Guttman, A. Rapid N-Glycan Release from Glycoproteins Using Immobilized PNGase F Microcolumns. *J. Chromatogr. B: Anal. Technol. Biomed. Life Sci.* **2016**, *1032*, 139−143.
(66) Thiesler, C. T.; Cajic, S.; Hoffmann, D.; Thiel, C.; van Diepen, L.; Hennig, R.; Sgodda, M.; Weiβmann, R.; Reichl, U.; Steinemann, D.; et al. Glycomic Characterization of Induced Pluripotent Stem Cells Derived from a Patient Suffering from Phosphomannomutase 2 Congenital Disorder of Glycosylation (PMM2-CDG). *Mol. Cell. Proteomics* **2016**, *15*, 1435−1452.
(67) Váradi, C.; Hóllo, Z.; Póliska, S.; Nagy, L.; Szekanecz, Z.; Váncsa, A.; Palatka, K.; Guttman, A. Combination of IgG N-Glycomics and Corresponding Transcriptomics Data to Identify Anti-TNF-α Treatment Responders in Inflammatory Diseases. *Electrophoresis* **2015**, *36*, 1330−1335.
(68) Vermassen, T.; Van Praet, C.; Vanderschaeghe, D.; Maenhout, T.; Lumen, N.; Callewaert, N.; Hoebeke, P.; Van Belle, S.; Rottey, S.; Delanghe, J. Capillary Electrophoresis of Urinary Prostate Glycoproteins Assists in the Diagnosis of Prostate Cancer. *Electrophoresis* **2014**, *35*, 1017−1024.
(69) Hennig, R.; Rapp, E.; Kottler, R.; Cajic, S.; Borowiak, M.; Reichl, U. In *Carbohydrate-Based Vaccines: Methods and Protocols*; Lepenies, B., Ed.; Humana Press: New York, NY, 2015, *1331*, 123−143.
(70) Jooß, K.; Sommer, J.; Bunz, S.-C.; Neusüß, C. In-Line SPE-CE Using a Fritless Bead String Design—Application for the Analysis of Organic Sulfonates Including Inline SPE-CE-MS for APTS-Labeled Glycans. *Electrophoresis* **2014**, *35*, 1236−1243.
(71) Laukens, B.; De Wachter, C.; Callewaert, N. In *Glyco-Engineering: Methods and Protocols*; Castilho, A., Ed.; Humana Press: New York, NY, 2015, *1321*, 103−122.
(72) O'Regan, N. L.; Steinfelder, S.; Schwedler, C.; Rao, G. B.; Srikantam, A.; Blanchard, V.; Hartmann, S. Filariasis Asymptomatically Infected Donors Have Lower Levels of Disialylated IgG Compared to Endemic Normals. *Parasite Immunol.* **2014**, *36*, 713−720.
(73) Wang, M.; Fang, M.; Zhu, J.; Feng, H.; Warner, E.; Yi, C.; Ji, J.; Gu, X.; Gao, C. Serum N-Glycans Outperform CA19−9 in Diagnosis of Extrahepatic Cholangiocarcinoma. *Electrophoresis* **2017**, *38*, 2749−2756.
(74) Ruhaak, L. R.; Zauner, G.; Huhn, C.; Bruggink, C.; Deelder, A. M.; Wuhrer, M. Glycan Labeling Strategies and Their Use in Identification and Quantification. *Anal. Bioanal. Chem.* **2010**, *397*, 3457−3481.
(75) Uematsu, R.; Furukawa, J.-i.; Nakagawa, H.; Shinohara, Y.; Deguchi, K.; Monde, K.; Nishimura, S.-I. High Throughput Quantitative Glycomics and Glycoform-Focused Proteomics of Murine Dermis and Epidermis. *Mol. Cell. Proteomics* **2005**, *4*, 1977−1989.
(76) Iwatsuka, K.; Iwamoto, H.; Kinoshita, M.; Inada, K.; Yasueda, S.-i.; Kakehi, K. Comparative Studies of N-Glycans and Glycosaminoglycans Present in SIRC (Statens Seruminstitut Rabbit Cornea) Cells and Corneal Epithelial Cells from Rabbit Eyes. *Curr. Eye Res.* **2014**, *39*, 686−694.
(77) Gattu, S.; Crihfield, C. L.; Holland, L. A. Microscale Measurements of Michaelis−Menten Constants of Neuraminidase with Nanogel Capillary Electrophoresis for the Determination of the Sialic Acid Linkage. *Anal. Chem.* **2017**, *89*, 929−936.
(78) Váradi, C.; Mittermayr, S.; Millán-Martín, S.; Bones, J. Quantitative Twoplex Glycan Analysis Using $^{12}C_6$ and $^{13}C_6$ Stable Isotope 2-Aminobenzoic Acid Labelling and Capillary Electrophoresis Mass Spectrometry. *Anal. Bioanal. Chem.* **2016**, *408*, 8691−8700.
(79) Yamamoto, S.; Nagai, E.; Asada, Y.; Kinoshita, M.; Suzuki, S. A Rapid and Highly Sensitive Microchip Electrophoresis of Mono- and Mucin-Type Oligosaccharides Labeled with 7-Amino-4-Methylcoumarin. *Anal. Bioanal. Chem.* **2015**, *407*, 1499−1503.
(80) Yodoshi, M.; Ikeda, N.; Yamaguchi, N.; Nagata, M.; Nishida, N.; Kakehi, K.; Hayakawa, T.; Suzuki, S. A Novel Condition for Capillary Electrophoretic Analysis of Reductively Aminated Saccharides without Removal of Excess Reagents. *Electrophoresis* **2013**, *34*, 3198−3205.
(81) Song, X.; Ju, H.; Lasanajak, Y.; Kudelka, M. R.; Smith, D. F.; Cummings, R. D. Oxidative Release of Natural Glycans for Functional Glycomics. Nat. *Nat. Methods* **2016**, *13*, 528−534.
(82) Mittermayr, S.; Guttman, A. Influence of Molecular Configuration and Conformation on the Electromigration of Oligosaccharides in Narrow Bore Capillaries. *Electrophoresis* **2012**, *33*, 1000−1007.
(83) Guttman, A.; Chen, F.-T. A.; Evangelista, R. A. Separation of 1-Aminopyrene-3,6,8-Trisulfonic-Labeled Asparagine-Linked Fetuin Glycans by Capillary Electrophoresis. *Electrophoresis* **1996**, *17*, 412−417.
(84) Guttman, A.; Herrick, S. Effect of the Quantity and Linkage Position of Mannose(α1,2) Residues in Capillary Gel Electrophoresis of High-Mannose-Type Oligosaccharides. *Anal. Biochem.* **1996**, *235*, 236−239.
(85) Jarvas, G.; Szigeti, M.; Chapman, J.; Guttman, A. Triple-Internal Standard Based Glycan Structural Assignment Method for Capillary Electrophoresis Analysis of Carbohydrates. *Anal. Chem.* **2016**, *88*, 11364−11367.
(86) https://lendulet.uni-pannon.hu/index.php/tools, accessed October 30, 2017.
(87) Szigeti, M.; Guttman, A. High-Resolution Glycan Analysis by Temperature Gradient Capillary Electrophoresis. *Anal. Chem.* **2017**, *89*, 2201−2204.

DOI: 10.1021/acs.chemrev.7b00669
Chem. Rev. 2018, 118, 7867−7885

(88) Hennig, R.; Cajic, S.; Borowiak, M.; Hoffmann, M.; Kottler, R.; Reichl, U.; Rapp, E. Towards Personalized Diagnostics via Longitudinal Study of the Human Plasma N-Glycome. *Biochim. Biophys. Acta, Gen. Subj.* **2016**, *1860*, 1728−1738.
(89) Behne, A.; Muth, T.; Borowiak, M.; Reichl, U.; Rapp, E. glyXalign: High-Throughput Migration Time Alignment Preprocessing of Electrophoretic Data Retrieved via Multiplexed Capillary Gel Electrophoresis with Laser-Induced Fluorescence Detection-Based Glycoprofiling. *Electrophoresis* **2013**, *34*, 2311−2315.
(90) Guttman, A.; Ülfelder, K. W. Exoglycosidase Matrix-Mediated Sequencing of a Complex Glycan Pool by Capillary Electrophoresis. *J. Chromatogr. A* **1997**, *781*, 547−554.
(91) Bush, D. R.; Zang, L.; Belov, A. M.; Ivanov, A. R.; Karger, B. L. High Resolution CZE-MS Quantitative Characterization of Intact Biopharmaceutical Proteins: Proteoforms of Interferon-β1. *Anal. Chem.* **2016**, *88*, 1138−1146.
(92) Zhao, Y.-P.; Xu, X.-Y.; Fang, M.; Wang, H.; You, Q.; Yi, C.-H.; Ji, J.; Gu, X.; Zhou, P.-T.; Cheng, C.; Gao, C.-F. Decreased Core-Fucosylation Contributes to Malignancy in Gastric Cancer. *PLoS One* **2014**, *9*, No. e94536.
(93) Holland, L. A.; Gattu, S.; Crihfield, C. L.; Bwanali, L. Capillary Electrophoresis with Stationary Nanogel Zones of Galactosidase and *Erythrina cristagalli* Lectin for the Determination of β(1−3)-Linked Galactose in Glycans. *J. Chromatogr. A* **2017**, *1523*, 90−96.
(94) Alley, W. R.; Mann, B. F.; Novotny, M. V. High-Sensitivity Analytical Approaches for the Structural Characterization of Glycoproteins. *Chem. Rev.* **2013**, *113*, 2668−2732.
(95) Veillon, L.; Huang, Y.; Peng, W.; Dong, X.; Cho, B. G.; Mechref, Y. Characterization of Isomeric Glycan Structures by LC-MS/MS. *Electrophoresis* **2017**, *38*, 2100−2114.
(96) Yamagami, M.; Matsui, Y.; Hayakawa, T.; Yamamoto, S.; Kinoshita, M.; Suzuki, S. Plug-Plug Kinetic Capillary Electrophoresis for in-Capillary Exoglycosidase Digestion as a Profiling Tool for the Analysis of Glycoprotein Glycans. *J. Chromatogr. A* **2017**, *1496*, 157−162.
(97) Kinoshita, M.; Kakehi, K. Capillary-Based Lectin Affinity Electrophoresis for Interaction Analysis between Lectins and Glycans. *Methods Mol. Biol.* **2014**, *1200*, 131−146.
(98) Biacchi, M.; Gahoual, R.; Said, N.; Beck, A.; Leize-Wagner, E.; François, Y.-N. Glycoform Separation and Characterization of Cetuximab Variants by Middle-up Off-Line Capillary Zone Electrophoresis-Uv/Electrospray Ionization-Ms. *Anal. Chem.* **2015**, *87*, 6240−6250.
(99) Snyder, C. M.; Alley, W. R.; Campos, M. I.; Svoboda, M.; Goetz, J. A.; Vasseur, J. A.; Jacobson, S. C.; Novotny, M. V. Complementary Glycomic Analyses of Sera Derived from Colorectal Cancer Patients by Maldi-Tof-Ms and Microchip Electrophoresis. *Anal. Chem.* **2016**, *88*, 9597−9605.
(100) Mitra, I.; Snyder, C. M.; Zhou, X.; Campos, M. I.; Alley, W. R.; Novotny, M. V.; Jacobson, S. C. Structural Characterization of Serum N-Glycans by Methylamidation, Fluorescent Labeling, and Analysis by Microchip Electrophoresis. *Anal. Chem.* **2016**, *88*, 8965−8971.
(101) Biacchi, M.; Bhajun, R.; Saïd, N.; Beck, A.; François, Y. N.; Leize-Wagner, E. Analysis of Monoclonal Antibody by a Novel CE-UV/MALDI-MS Interface. *Electrophoresis* **2014**, *35*, 2986−2995.
(102) Kammeijer, G. S. M.; Jansen, B. C.; Kohler, I.; Heemskerk, A. A. M.; Mayboroda, O. A.; Hensbergen, P. J.; Schappler, J.; Wuhrer, M. Sialic Acid Linkage Differentiation of Glycopeptides Using Capillary Electrophoresis − Electrospray Ionization − Mass Spectrometry. *Sci. Rep.* **2017**, *7*, 3733.
(103) Jayo, R. G.; Thaysen-Andersen, M.; Lindenburg, P. W.; Haselberg, R.; Hankemeier, T.; Ramautar, R.; Chen, D. D. Y. Simple Capillary Electrophoresis−Mass Spectrometry Method for Complex Glycan Analysis Using a Flow-through Microvial Interface. *Anal. Chem.* **2014**, *86*, 6479−6486.
(104) Snyder, C. M.; Zhou, X.; Karty, J. A.; Fonslow, B. R.; Novotny, M. V.; Jacobson, S. C. Capillary Electrophoresis−Mass Spectrometry for Direct Structural Identification of Serum N-Glycans. *J. Chromatogr. A* **2017**, *1523*, 127−139.
(105) Zhong, X.; Chen, Z.; Snovida, S.; Liu, Y.; Rogers, J. C.; Li, L. Capillary Electrophoresis-Electrospray Ionization-Mass Spectrometry for Quantitative Analysis of Glycans Labeled with Multiplex Carbonyl-Reactive Tandem Mass Tags. *Anal. Chem.* **2015**, *87*, 6527−6534.
(106) Busnel, J.-M.; Schoenmaker, B.; Ramautar, R.; Carrasco-Pancorbo, A.; Ratnayake, C.; Feitelson, J. S.; Chapman, J. D.; Deelder, A. M.; Mayboroda, O. A. High Capacity Capillary Electrophoresis-Electrospray Ionization Mass Spectrometry: Coupling a Porous Sheathless Interface with Transient-Isotachophoresis. *Anal. Chem.* **2010**, *82*, 9476−9483.
(107) Khatri, K.; Klein, J. A.; Haserick, J. R.; Leon, D. R.; Costello, C. E.; McComb, M. E.; Zaia, J. Microfluidic Capillary Electrophoresis−Mass Spectrometry for Analysis of Monosaccharides, Oligosaccharides, and Glycopeptides. *Anal. Chem.* **2017**, *89*, 6645−6655.
(108) Hahne, H.; Neubert, P.; Kuhn, K.; Etienne, C.; Bomgarden, R.; Rogers, J. C.; Kuster, B. Carbonyl-Reactive Tandem Mass Tags for the Proteome-Wide Quantification of N-Linked Glycans. *Anal. Chem.* **2012**, *84*, 3716−3724.
(109) Dube, D. H.; Bertozzi, C. R. Glycans in Cancer and Inflammation - Potential for Therapeutics and Diagnostics. *Nat. Rev. Drug Discovery* **2005**, *4*, 477−488.
(110) Gornik, O.; Wagner, J.; Pučić, M.; Knežević, A.; Redžić, I.; Lauc, G. Stability of N-Glycan Profiles in Human Plasma. *Glycobiology* **2009**, *19*, 1547−1553.
(111) Pučić, M.; Knežević, A.; Vidič, J.; Adamczyk, B.; Novokmet, M.; Polašek, O.; Gornik, O.; Šupraha-Goreta, S.; Wormald, M. R.; Redžić, I.; et al. High Throughput Isolation and Glycosylation Analysis of IgG−Variability and Heritability of the IgG Glycome in Three Isolated Human Populations. *Mol. Cell. Proteomics* **2011**, *10* (1−15), M111.010090.
(112) Vanhooren, V.; Dewaele, S.; Libert, C.; Engelborghs, S.; De Deyn, P. P.; Toussaint, O.; Debacq-Chainiaux, F.; Poulain, M.; Glupczynski, Y.; Franceschi, C.; et al. Serum N-Glycan Profile Shift During Human Ageing. *Exp. Gerontol.* **2010**, *45*, 738−743.
(113) Maverakis, E.; Kim, K.; Shimoda, M.; Gershwin, M. E.; Patel, F.; Wilken, R.; Raychaudhuri, S.; Ruhaak, L. R.; Lebrilla, C. B. Glycans in the Immune System and the Altered Glycan Theory of Autoimmunity: A Critical Review. *J. Autoimmun.* **2015**, *57*, 1−13.
(114) Adamczyk, B.; Tharmalingam, T.; Rudd, P. M. Glycans as Cancer Biomarkers. *Biochim. Biophys. Acta, Gen. Subj.* **2012**, *1820*, 1347−1353.
(115) Peracaula, R.; Barrabés, S.; Sarrats, A.; Rudd, P. M.; de Llorens, R. Altered Glycosylation in Tumours Focused to Cancer Diagnosis. Dis. *Dis. Markers* **2008**, *25*, 207−218.
(116) Fuster, M. M.; Esko, J. D. The Sweet and Sour of Cancer: Glycans as Novel Therapeutic Targets. *Nat. Rev. Cancer* **2005**, *5*, 526−542.
(117) de Leoz, M. L. A.; Young, L. J. T.; An, H. J.; Kronewitter, S. R.; Kim, J.; Miyamoto, S.; Borowsky, A. D.; Chew, H. K.; Lebrilla, C. B. High-Mannose Glycans Are Elevated During Breast Cancer Progression. *Mol. Cell. Proteomics* **2011**, *10*, M110.002717.
(118) Miyoshi, E.; Moriwaki, K.; Nakagawa, T. Biological Function of Fucosylation in Cancer Biology. *J. Biochem.* **2008**, *143*, 725−729.
(119) Dennis, J. W.; Granovsky, M.; Warren, C. E. Glycoprotein Glycosylation and Cancer Progression. *Biochim. Biophys. Acta, Gen. Subj.* **1999**, *1473*, 21−34.
(120) Balmaña, M.; Giménez, E.; Puerta, A.; Llop, E.; Figueras, J.; Fort, E.; Sanz-Nebot, V.; de Bolós, C.; Rizzi, A.; Barrabés, S.; et al. Increased α1−3 Fucosylation of α-1-Acid Glycoprotein (AGP) in Pancreatic Cancer. *J. Proteomics* **2016**, *132*, 144−154.
(121) Weiz, S.; Wieczorek, M.; Schwedler, C.; Kaup, M.; Braicu, E. I.; Sehouli, J.; Tauber, R.; Blanchard, V. Acute-Phase Glycoprotein N-Glycome of Ovarian Cancer Patients Analyzed by CE-LIF. *Electrophoresis* **2016**, *37*, 1461−1467.
(122) Robajac, D.; Masnikosa, R.; Vanhooren, V.; Libert, C.; Miković, Ž.; Nedić, O. The N-Glycan Profile of Placental Membrane Glycoproteins Alters During Gestation and Aging. *Mech. Ageing Dev.* **2014**, *138*, 1−9.

DOI: 10.1021/acs.chemrev.7b00669
Chem. Rev. 2018, 118, 7867−7885

(123) Konze, S. A.; Cajic, S.; Oberbeck, A.; Hennig, R.; Pich, A.; Rapp, E.; Buettner, F. F. R. Quantitative Assessment of Sialo-Glycoproteins and N-Glycans During Cardiomyogenic Differentiation of Human Induced Pluripotent Stem Cells. *ChemBioChem* **2017**, *18*, 1317−1331.
(124) Zhang, L.; Lawson, K.; Yeung, B.; Wypych, J. Capillary Zone Electrophoresis Method for a Highly Glycosylated and Sialylated Recombinant Protein: Development, Characterization and Application for Process Development. *Anal. Chem.* **2015**, *87*, 470−476.
(125) Gahoual, R.; Biacchi, M.; Chicher, J.; Kuhn, L.; Hammann, P.; Beck, A.; Leize-Wagner, E.; François, Y. N. Monoclonal Antibodies Biosimilarity Assessment Using Transient Isotachophoresis Capillary Zone Electrophoresis-Tandem Mass Spectrometry. *mAbs* **2014**, *6*, 1464−1473.
(126) Redman, E. A.; Mellors, J. S.; Starkey, J. A.; Ramsey, J. M. Characterization of Intact Antibody Drug Conjugate Variants Using Microfluidic Capillary Electrophoresis−Mass Spectrometry. *Anal. Chem.* **2016**, *88*, 2220−2226.
(127) Redman, E. A.; Ramos-Payan, M.; Mellors, J. S.; Ramsey, J. M. Analysis of Hemoglobin Glycation Using Microfluidic Ce-Ms: A Rapid, Mass Spectrometry Compatible Method for Assessing Diabetes Management. *Anal. Chem.* **2016**, *88*, 5324−5330.
(128) Guerrini, M.; Beccati, D.; Shriver, Z.; Naggi, A.; Viswanathan, K.; Bisio, A.; Capila, I.; Lansing, J. C.; Guglieri, S.; Fraser, B.; et al. Oversulfated Chondroitin Sulfate Is a Contaminant in Heparin Associated with Adverse Clinical Events. *Nat. Biotechnol.* **2008**, *26*, 669−675.
(129) Liu, H.; Zhang, Z.; Linhardt, R. J. Lessons Learned from the Contamination of Heparin. *Nat. Prod. Rep.* **2009**, *26*, 313−321.
(130) Sun, X.; Lin, L.; Liu, X.; Zhang, F.; Chi, L.; Xia, Q.; Linhardt, R. J. Capillary Electrophoresis−Mass Spectrometry for the Analysis of Heparin Oligosaccharides and Low Molecular Weight Heparin. *Anal. Chem.* **2016**, *88*, 1937−1943.
(131) Lin, L.; Liu, X.; Zhang, F.; Chi, L.; Amster, I. J.; Leach, F. E.; Xia, Q.; Linhardt, R. J. Analysis of Heparin Oligosaccharides by Capillary Electrophoresis−Negative-Ion Electrospray Ionization Mass Spectrometry. *Anal. Bioanal. Chem.* **2017**, *409*, 411−420.
(132) Maccari, F.; Galeotti, F.; Zampini, L.; Padella, L.; Tomanin, R.; Concolino, D.; Fiumara, A.; Galeazzi, T.; Coppa, G.; Gabrielli, O.; et al. Total and Single Species of Uronic Acid-Bearing Glycosaminoglycans in Urine of Newborns of 2−3 days of Age for Early Diagnosis Application. *Clin. Chim. Acta* **2016**, *463*, 67−72.
(133) Ucakturk, E.; Cai, C.; Li, L.; Li, G.; Zhang, F.; Linhardt, R. J. Capillary Electrophoresis for Total Glycosaminoglycan Analysis. *Anal. Bioanal. Chem.* **2014**, *406*, 4617−4626.
(134) Zhao, T.; Song, X.; Tan, X.; Xu, L.; Yu, M.; Wang, S.; Liu, X.; Wang, F. Development of a Rapid Method for Simultaneous Separation of Hyaluronic Acid, Chondroitin Sulfate, Dermatan Sulfate and Heparin by Capillary Electrophoresis. *Carbohydr. Polym.* **2016**, *141*, 197−203.
(135) Restaino, O. F.; di Lauro, I.; Di Nuzzo, R.; De Rosa, M.; Schiraldi, C. New Insight into Chondroitin and Heparosan-Like Capsular Polysaccharide Synthesis by Profiling of the Nucleotide Sugar Precursors. *Biosci. Rep.* **2017**, *37* (1−11), BSR20160548.
(136) Witos, J.; Samuelsson, J.; Cilpa-Karhu, G.; Metso, J.; Jauhiainen, M.; Riekkola, M.-L. Partial Filling Affinity Capillary Electrophoresis Including Adsorption Energy Distribution Calculations - Towards Reliable and Feasible Biomolecular Interaction Studies. *Analyst* **2015**, *140*, 3175−3182.
(137) Liang, A.; Desai, U. R. In *Glycosaminoglycans: Chemistry and Biology*; Balagurunathan, K., Nakato, H., Desai, U. R., Eds.; Humana Press: New York, NY, 2015, *1229*, 355−375.
(138) Oliveira, D. L.; et al. Natural Caprine Whey Oligosaccharides Separated by Membrane Technology and Profile Evaluation by Capillary Electrophoresis. *Food Bioprocess Technol.* **2014**, *7*, 915−920.
(139) Lu, Y.; Hu, Y.; Wang, T.; Yang, X.; Zhao, Y. Rapid Determination and Quantitation of Compositional Carbohydrates to Identify Honey by Capillary Zone Electrophoresis. *CyTA–J. Food* **2017**, *15*, 531−537.
(140) Gatea, F.; et al. Chemical Constituents and Bioactive Potential of Portulaca Pilosa L Vs. Portulaca Oleracea L. *Med. Chem. Res.* **2017**, *26*, 1516−1527.
(141) Dominguez, M. A.; Jacksén, J.; Emmer, Å.; Centurión, M. E. Capillary Electrophoresis Method for the Simultaneous Determination of Carbohydrates and Proline in Honey Samples. *Microchem. J.* **2016**, *129*, 1−4.
(142) Toutounji, M. R.; Van Leeuwen, M. P.; Oliver, J. D.; Shrestha, A. K.; Castignolles, P.; Gaborieau, M. Quantification of Sugars in Breakfast Cereals Using Capillary Electrophoresis. *Carbohydr. Res.* **2015**, *408*, 134−141.
(143) Navarro-Pascual-Ahuir, M.; Lerma-García, M. J.; Simó-Alfonso, E. F.; Herrero-Martínez, J. M. Rapid Differentiation of Commercial Juices and Blends by Using Sugar Profiles Obtained by Capillary Zone Electrophoresis with Indirect UV Detection. *J. Agric. Food Chem.* **2015**, *63*, 2639−2646.
(144) Alinat, E.; Jemmali, S.; Delaunay, N.; Archer, X.; Gareil, P. Analysis of Underivatized Cellodextrin Oligosaccharides by Capillary Electrophoresis with Direct Photochemically Induced UV-Detection. *Electrophoresis* **2015**, *36*, 1555−1563.
(145) Moreno, D.; Berli, F.; Bottini, R.; Piccoli, P. N.; Silva, M. F. Grapevine Tissues and Phenology Differentially Affect Soluble Carbohydrates Determination by Capillary Electrophoresis. *Plant Physiol. Biochem.* **2017**, *118*, 394−399.
(146) Francisco, K. J. M.; do Lago, C. L. A Capillary Electrophoresis System with Dual Capacitively Coupled Contactless Conductivity Detection and Electrospray Ionization Tandem Mass Spectrometry. *Electrophoresis* **2016**, *37*, 1718−1724.
(147) Mar, N. N.; Umemoto, T.; Abdulah, S. N. A.; Maziah, M. Chain Length Distribution of Amylopectin and Physicochemical Properties of Starch in Myanmar Rice Cultivars. *Int. J. Food Prop.* **2015**, *18*, 1719−1730.
(148) Wu, A. C.; Li, E.; Gilbert, R. G. Exploring Extraction/Dissolution Procedures for Analysis of Starch Chain-Length Distributions. *Carbohydr. Polym.* **2014**, *114*, 36−42.
(149) Bai, Y.; Wu, P.; Wang, K.; Li, C.; Li, E.; Gilbert, R. G. Effects of Pectin on Molecular Structural Changes in Starch During Digestion. *Food Hydrocolloids* **2017**, *69*, 10−18.
(150) Yu, W.; Tan, X.; Zou, W.; Hu, Z.; Fox, G. P.; Gidley, M. J.; Gilbert, R. G. Relationships between Protein Content, Starch Molecular Structure and Grain Size in Barley. *Carbohydr. Polym.* **2017**, *155*, 271−279.
(151) Ibrahim, Y. M.; Hamid, A. M.; Deng, L.; Garimella, S. V. B.; Webb, I. K.; Baker, E. S.; Smith, R. D. New Frontiers for Mass Spectrometry Based Upon Structures for Lossless Ion Manipulations. *Analyst* **2017**, *142*, 1010−1021.
(152) Szigeti, M.; Guttman, A. Automated N-Glycosylation Sequencing of Biopharmaceuticals by Capillary Electrophoresis. *Sci. Rep.* **2017**, *7*, 11663.
(153) Redman, E. A.; Batz, N. G.; Mellors, J. S.; Ramsey, J. M. Integrated Microfluidic Capillary Electrophoresis-Electrospray Ionization Devices with Online MS Detection for the Separation and Characterization of Intact Monoclonal Antibody Variants. *Anal. Chem.* **2015**, *87*, 2264−2272.
(154) Szarka, M.; Guttman, A. Smartphone Cortex Controlled Real-Time Image Processing and Reprocessing for Concentration Independent LED Induced Fluorescence Detection in Capillary Electrophoresis. *Anal. Chem.* **2017**, *89*, 10673−10678.

DOI: 10.1021/acs.chemrev.7b00669
Chem. Rev. 2018, 118, 7867−7885